THE UNIVERSITY OF ALBERTA

RELEASE FORM

NAME OF AUTHOR DWIGHT LEROY ADAMS

TITLE OF THESIS APPARATUS DESIGN FOR THE SIMULTANEOUS INVESTIGATION
OF FLUID FLOW BETWEEN PARALLEL PLATES WITH SURFACE
SOLIDIFICATION

DEGREE FOR WHICH THESIS WAS PRESENTED MASTER OF SCIENCE

YEAR THIS DEGREE GRANTED [illegible]

Permission is hereby granted to THE UNIVERSITY OF
ALBERTA LIBRARY to reproduce single copies of [illegible]

THE UNIVERSITY OF ALBERTA

RELEASE FORM

NAME OF AUTHOR DWIGHT LEROY ADAMIC

TITLE OF THESIS APPARATUS DESIGN FOR THE EXPERIMENTAL INVESTIGATION OF FLUID FLOW BETWEEN PARALLEL PLATES WITH SURFACE SOLIDIFICATION

DEGREE FOR WHICH THESIS WAS PRESENTED MASTER OF SCIENCE

YEAR THIS DEGREE GRANTED 1973

THE UNIVERSITY OF ALBERTA

APPARATUS DESIGN FOR THE EXPERIMENTAL INVESTIGATION OF FLUID FLOW BETWEEN PARALLEL PLATES WITH SURFACE SOLIDIFICATION

by

Ⓒ DWIGHT LEROY ADAMIC

A THESIS
SUBMITTED TO THE FACULTY OF GRADUATE STUDIES AND RESEARCH
IN PARTIAL FULFILMENT OF THE REQUIREMENTS FOR THE DEGREE
OF MASTER OF SCIENCE

DEPARTMENT OF MECHANICAL ENGINEERING

EDMONTON, ALBERTA

FALL, 1973

THE UNIVERSITY OF ALBERTA

FACULTY OF GRADUATE STUDIES AND RESEARCH

The undersigned certify that they have read, and recommend to the Faculty of Graduate Studies and Research, for acceptance, a thesis entitled "Apparatus Design for the Experimental Investigation of Fluid Flow Between Parallel Plates With Surface Solidification" submitted by Dwight Leroy Adamic in partial fulfilment of the requirements for the degree of Master of Science.

ABSTRACT

A design is presented for the experimental investigation of the transient growth of an ice layer that forms when superheated water flows, under conditions of constant head, between two parallel plates. Both plates are insulated but for a portion of one which is convectively cooled to a temperature below the freezing point of water. A mathematical formulation is proposed for the case when the water flow is vertical. The experimental procedure and method of testing is outlined.

ACKNOWLEDGEMENTS

Thanks would like to be extended to the following:

- Dr. C. M. Rodkiewicz for his guidance and supervision of the thesis.
- Dr. W. A. Wolfe for suggesting the thesis topic.
- To all members of the Mechanical Engineering Technical Staff for the construction, assembly and preliminary testing of the apparatus.
- To the author's mother-in-law, Mrs. A. Kuzio for typing the thesis.
- To the National Research Council for financial support.
- To Connie for her understanding.

TABLE OF CONTENTS

LIST OF FIGURES

NOMENCLATURE

C	specific heat
d	distance between parallel plates
Eu	Euler number = $\frac{Pc}{\rho_L U_c^2}$
Fr	Froude number = $\frac{Um^2}{dg}$
g	gravitational acceleration
h	heat transfer coefficient
ℓ	length of the freezing zone
L	latent heat
p	pressure
P	dimensionless pressure = $\frac{p - pe}{\rho_L Um^2}$
Pe	Péclèt number = Re• Pr = $\frac{Umd}{\alpha_L}$
Pr	Prandtl number = $\frac{\upsilon}{\alpha_L}$
Re	Reynolds number = $\frac{Umd}{\upsilon}$
s_f	fully developed solid thickness
Ste	Stefan number = $C_s(To - Tf)/L$
t	time coordinate
T	temperature
u	axial velocity
U	dimensionless axial velocity = $\frac{U}{Um}$
Um	average velocity at time t = 0

v	transverse velocity
V	dimensionless transverse velocity = $\frac{v\ell}{Umd}$
x	axial direction
X	dimensionless axial direction = $\frac{x}{\ell}$
y	transverse direction
Y	dimensionless transverse direction = $\frac{y}{d}$
y_i	interface position
α	thermal diffusivity ratio = $\frac{\alpha_L}{\alpha_s}$
κ	thermal conductivity ratio = $\frac{\kappa_L}{\kappa_s}$
δ	scale factor = $\frac{d}{\ell}$
η	dimensionless interface position = $\frac{y}{d}$
ρ	density ratio = ρ_s/ρ_L
μ	absolute viscosity
σ	superheat ratio = $\frac{Tf - Tw}{To - Tf}$
θ	dimensionless temperature of the liquid $\frac{T_L - Tf}{To - Tf}$
θ	dimensionless temperature of the solid $\frac{Ts - Tf}{Tf - Tw}$
υ	kinematic viscosity
τ	dimensionless time coordinate = $\frac{\alpha_s t}{d^2}$
Φ	dimensionless dissipation function

Subscripts

b	bulk temperature
c	character scale factor
e	exit condition
f	fusion condition, final condition
i	interface condition, initial condition
L	liquid state
m	average or mean value
0	inlet condition
s	solid state

Superscripts

$'$	normalized quantity

CHAPTER 1

INTRODUCTION

1.1. Statement of Objectives

An important class of heat transfer problems involves solidification or melting. Deemed free boundary problems, they are characterized by a moving liquid-solid interface whose boundary condition is nonlinear and whose position is not known 'a priori' but must be determined as part of the solution. For internal flow problems the difficulty in obtaining an analytic solution is further compounded, since the liquid phase is directly affected by the interface motion. This results in a coupling of the field equations in both phases unless one of the phases can be assumed to be at the fusion temperature.

The study presented in this thesis is the development of an experimental apparatus which will be used to investigate the transient solidification of water flowing through a parallel plate test section. One of the plates is insulated while the other is cooled to temperatures below the freezing point. A system, comprised in part of this test section, has a constant pressure drop applied across it. As freezing progresses with time the pressure drop in the test section increases, while the remainder of the system experiences a decrease in the pressure drop and a corresponding decrease in the flow rate. Conditions under which an ice barrier can be grown into the fluid stream need to be examined and efforts made to predict the pressure drop required to prevent the test section from freezing shut. In this regard an experimental apparatus has been designed and constructed so that data such as the history of the ice-water interface for various test

conditions can be obtained.

1.2 Review of Revelant Literature

The first published discussion of a heat conduction problem involving freezing or melting was by Stefan [1]. Since then numerous mathematical studies have been undertaken as evidenced by the literature review of Muehlbauer and Sunderland [2]. Due to the difficulties outlined in Section 1.1, few exact solutions for the transient frozen layer thickness and temperature distributions have been found. Most of these are summarized by Carslaw and Jaeger [3].

One area of research which until recent years has received little attention involves solidification or melting on a surface exposed to fluid flow. Brush [4] in 1916 discussed ice formation in water mains. He noted that the ice thickness is dependent upon the water temperature, flow rate and wall temperature, but presented no theoretical analysis or experimental data. Hirschberg [5] studied flow through a pipe whose wall temperature was maintained below the freezing temperature of the liquid. Assuming a constant pressure drop maintained between the inlet and outlet of the pipe, a relationship between the parameters for steady-state conditions and a uniform solid phase thickness was derived.

Libby and Chen [6] presented an approximate analysis for "short" and "long" times for the growth of a solid layer deposited on a cold surface by a flowing gas. The solution was based on the integral method as proposed by Goodman [7, 8, 9]. Lapadula and Mueller [10] arrived at a simpler solution to the same problem by employing the variational technique developed by Biot [11, 12].

Yang [13] studied the unsteady formation of ice on an instantaneously cooled plate subjected to plane stagnation flow of an isothermal liquid. A "short" time solution was derived by asymptotic series expansions, while the "long" time solution based on first-order deviations from steady-state conditions was obtained by Laplace transforms. The mathematical procedure is complicated and application to other problems would likely increase the complexity.

Beaubouef and Chapman [14] used a similarity analysis employing a finite difference technique to give the thickness of a solid deposited by a flowing liquid on a cold surface as a function of time and position. Zerkle and Sunderland [15] investigated the heat transfer and pressure drop effects of steady state liquid solidification at the inner surface of a circular pipe. Unlike Hirschberg [5] a uniform solid-phase shell thickness was not assumed. It was argued that the axial velocity would retain its parabolic profile throughout the cooling region. By assuming this form, and by use of suitable nondimensional variables the problem was shown to reduce to the classical Graetz problem. Experimental observations taken with water flowing through horizontal tubes showed that free convection may produce considerable deviation from the theoretical results.

Lee and Zerkle [16] then extended Zerkle and Sunderland's earlier work to steady-state liquid solidification in a parallel plate channel. By assuming a parabolic velocity distribution in the channel and transforming the heat conduction equation, a solution was obtained by separation of variables. The resulting dimensionless interface distance was obtained by successive substitution into the interface equation.

Siegel and Savino [17] considered a warm flowing medium solidifying onto a plate convectively cooled on the underside. Three distinct analytic solutions were obtained: (a) an analytical iterative procedure, similar to that developed by Adams [18] , which essentially converged to the exact solution on the third iteration, but which increased in complexity with each new iteration; (b) by employing a second order polynomial approximation for the temperature in conjunction with Goodman's integral technique [7, 8, 9] ; (c) and by applying the integral technique and approximate temperature profile to the interface equation. Experimental values of ice thickness and plate surface temperature throughout the transient and steady-state growth period generally agreed favorably with the theoretically predicted values, except that under some conditions the subcooling of the frozen layer during its formation slowed the growth rate substantially. To investigate this effect further Siegel and Savino [19] again considered a medium flowing over a plate convectively cooled on the underside, but included the heat capacities of both the frozen layer and the plate in their analysis. The frozen layer growth was obtained by integrating the transient heat conduction equation within both the frozen layer and wall. This gave coupled integral equations for the temperature distributions in both media and an integral equation for the frozen layer growth. The solution to this set of equations was then iteratively obtained and agreed well with the experimental observations. Savino and Siegel [20] then applied their analytic iterative technique developed earlier to a warm liquid flowing over an isothermal plate. It was found possible to carry out a fourth iteration which

again essentially converged to the exact solution and which showed good agreement with Libby and Chen [6], Lapadula and Mueller [10], and Beaubouef and Chapman [14].

Gort [21] studied analytically and experimentally the freezing problem inside a vertical cylinder both with and without forced flow. An approximate solution was derived for a fluid whose temperature was at its freezing point and which flowed through a cylinder whose wall temperature was maintained below freezing.

DesRuisseaux and Zerkle [22] developed a technique which predicted conditions under which a hydraulic system freezes shut. The system pressure drop was analytically determined as a function of Reynold's number at steady-state conditions for various wall temperatures. The minimum pressure drop to stop the system from freezing shut was specified.

Ozisik and Mulligan [23] investigated analytically the transient freezing of a liquid flowing inside a circular tube. The restricting assumptions were:

a) the tube wall temperature was lower than freezing
b) slug flow velocity profile
c) the variation of the thickness of the solid layer with both time and position was small so that a quasisteady state heat conduction in the solid phase could be assumed.

The method of solution involved determination of the dimensionless liquid and solid phase temperatures in terms of the unknown dimensionless solid-liquid interface radius. The equations were coupled to the interface equation to obtain a single ordinary differential equation for the interface radius which was then solved to give the interface

radius as a function of time and axial position.

Stephan [24] considered flow along a convectively cooled plate and through a convectively cooled pipe. A parabolic temperature distribution was assumed for the solid phase matching all the wall boundary conditions but satisfying the energy equation at the solid-liquid interface only. An interesting outcome of the analysis was that in pipe flow, growth of the solid layer could stop at two critical points for certain values of the ambient heat transfer and the convective heat flux at the solid-liquid interface. One of these points was a stable condition, the other unstable; both however, were dependent on the preceeding history of the solid phase as to their stability.

Freeborn [25, 26] presented a theoretical and experimental study of the transient growth of an ice layer formed as superheated water flowed through a convectively cooled vertical cylinder. The analysis considered two regions: an ice free zone where the fluid's superheat prevents ice formation, and an ice forming zone. Following the work of Sellars et al [27] the temperature profile at the entrance to the ice forming zone was obtained. By assuming the parabolic velocity profile used by Zerkle and Sunderland [15] which adjusts for local variations in the ice thickness, Freeborn derived an asymptotic solution for the temperature distribution in the ice and was able to predict the rate of solidification and its effect on the pressure drop.

Nyren [28, 29] extended the work of Freeborn [26] to include the effect produced by circumferential variations in the external heat flux as well as the sensible heat in the ice layer. A perturbation

expansion about the quasi-steady-state solution was found. The influence of the non-uniform convection on the interface profile was shown graphically for two cases. Experimental results for flow through a uniformly cooled and inclined pipe were given.

More recently, due to the complexity of the problems being investigated, solutions have tended to rely on numerical analysis. Bilenas and Jiji [30 , 31] presented both a variational and a numerical solution to the problem of axisymmetric fluid flow in tubes with surface solidification. The numerical solution was based on finite difference approximations of the continuity, momentum and energy equations with Lagrangian interpolation equations employed at the moving interface. The paper was unique since prior to its publication no numerical scheme was available which would solve two-dimensional fluid dynamics problems involving solidification. Effects such as viscous dissipation, axial viscous shear, axial conduction and discontinuity in the mass density due to phase change were included in the analysis.

Although not concerned with the field equations governing the liquid phase, the publications of Lazaridis [32] and Bruno [33] should be mentioned since both were concerned with transient multi-dimensional change of phase. Lazaridis devised one-, two- and three-dimensional finite difference schemes to solve the heat conduction equation for typical boundary conditions. Bruno treated the one- and two-dimensional heat conduction equations describing a finite body bounded by two insulated surfaces subjected to a known heat flux.

1.3 Applications

With the formation of ice and snow and the annual coming of spring, solidification and melting were known to earliest man. Today free boundary problems are encountered in such diverse areas as the freezing of foods, casting of metals, spacecraft propulsion systems, and the control of frost formation. Of particular concern to Canadians is the industrialization of the country's northern and arctic regions. Problems such as building pipelines through areas of permafrost, and failsafe heat and water supply systems for arctic cities require a thorough understanding of the freezing and melting process. This is of special importance if the environment of the region is to be preserved.

The application that motivated the present study is the possibility of controlling and stopping the flow of water by an essentially static means. Such a device which could function as a valve in part of a water piping system would have the advantage of involving a minimum of moving parts. This also reduces the sealing problems associated with the penetration of fluid boundaries by shafts or other devices.

CHAPTER II

MATHEMATICAL FORMULATION

2.1 Governing Equations

Consider a system where initially superheated water flows vertically upwards between two insulated parallel plates with a steady laminar motion. At some time, say $t = 0$, a portion of one of the plates has its temperature lowered to a subfusion value. Almost instantly a thin layer of ice forms on the surface of the cooled wall producing regions referred to as the adiabatic and freezing zones in figure 2.1. As time progresses the ice grows towards the opposing side until either blockage occurs or a steady-state profile is reached. During the freezing process the pressure drop across the system is maintained constant and the temperature distribution at the inlet to the freezing zone invariant.

If the flow through the freezing zone is assumed laminar, and the liquid Newtonian with constant properties (ρ_L, κ_L, C_L, μ); the differential equations governing the liquid phase in two dimensions are:

CONTINUITY EQUATION

$$\frac{\partial u}{\partial x} + \frac{\partial v}{\partial y} = 0 \qquad 2.1 - 1$$

EQUATIONS OF MOTION

x component

$$\rho_L \left\{ \frac{\partial u}{\partial t} + u \cdot \frac{\partial u}{\partial x} + v \cdot \frac{\partial u}{\partial y} \right\} = - \frac{\partial p}{\partial x} + \mu \left\{ \frac{\partial^2 u}{\partial x^2} + \frac{\partial^2 u}{\partial y^2} \right\} - \rho_L \cdot g_x \qquad 2.1 - 2$$

y component

$$\rho_L \left\{ \frac{\partial v}{\partial t} + u \cdot \frac{\partial v}{\partial x} + v \cdot \frac{\partial v}{\partial y} \right\} = - \frac{\partial p}{\partial y} + \mu \left\{ \frac{\partial^2 v}{\partial x^2} + \frac{\partial^2 v}{\partial y^2} \right\} \qquad 2.1 - 3$$

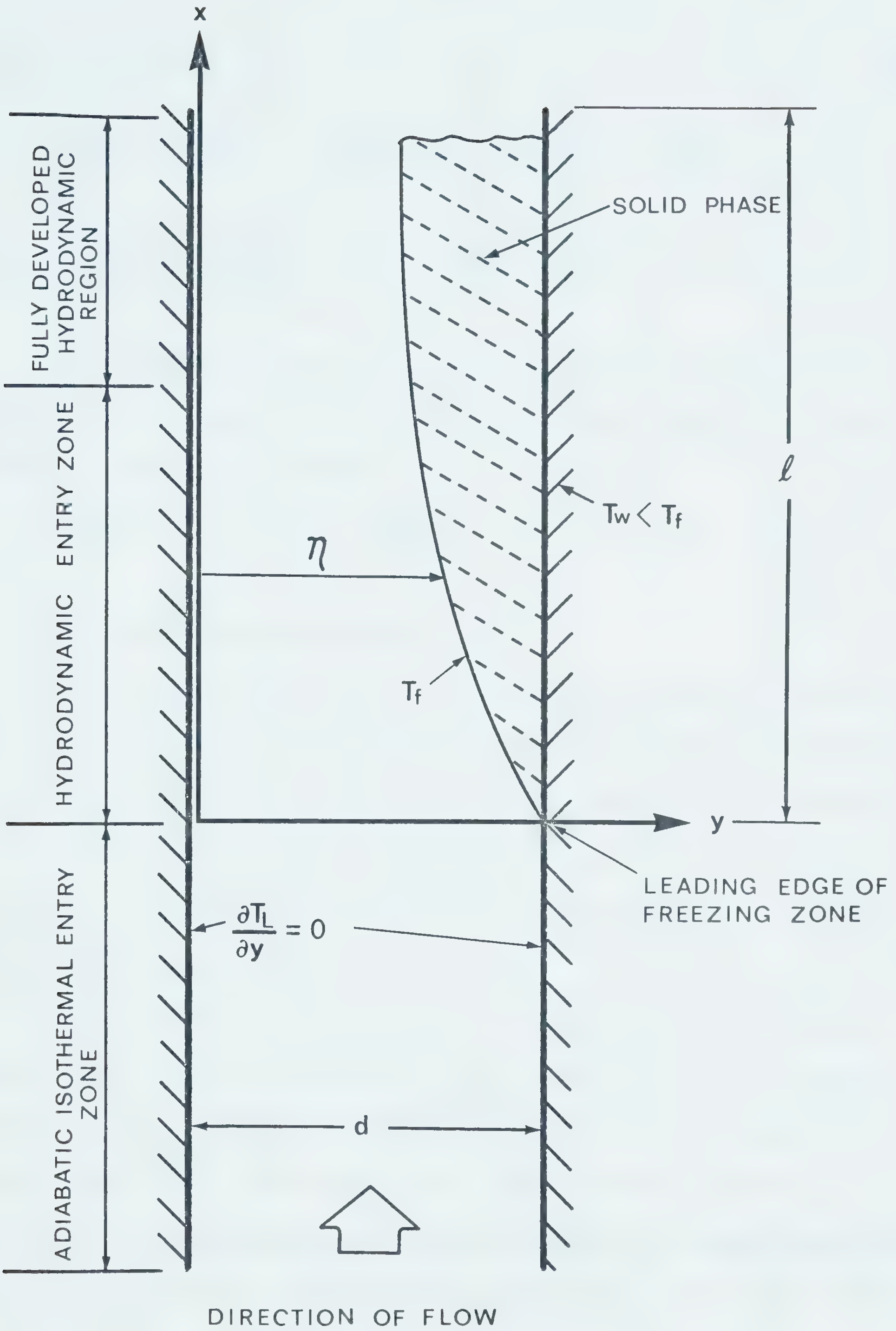

FIGURE 2.1 PARALLEL PLATE SYSTEM WITH SURFACE SOLIDIFICATION

ENERGY EQUATION

$$\rho_L C_L \left\{ \frac{\partial T_L}{\partial t} + u\cdot\frac{\partial T_L}{\partial x} + v\cdot\frac{\partial T_L}{\partial y} \right\} = \kappa_L \left\{ \frac{\partial^2 T_L}{\partial x^2} + \frac{\partial^2 T_L}{\partial y^2} \right\}$$

$$+ 2\mu \left\{ \left[\frac{\partial u}{\partial x}\right]^2 + \left[\frac{\partial v}{\partial y}\right]^2 \right\} + \mu \left\{ \frac{\partial u}{\partial y} + \frac{\partial v}{\partial x} \right\}^2 \qquad 2.1 - 4$$

If the material properties (ρ_s, κ_s, C_s) for the solid are also constant but not necessarily the same as the liquid phase the energy equation for the solid becomes:

$$\rho_s C_s \frac{\partial T_s}{\partial t} = \kappa_s \left\{ \frac{\partial^2 T_s}{\partial x^2} + \frac{\partial^2 T_s}{\partial y^2} \right\} \qquad 2.1 - 5$$

2.2 Order of Magnitude Analysis

The conditions under which the foregoing equations may be simplified can be obtained by non-dimensionalizing the equations in terms of dimensionless variables of unit order. This normalization procedure in addition produces dimensionless parameters essential for experimental simulation of the phenomena to be studied, for determination of the range of experimental data [34] .

The first step in the procedure is to normalize the governing equations by determining suitable scales or characteristic quantities which reduce the variables and their derivatives to non-dimensional form of unit order of magnitude. These characteristic quantities, chosen in accordance with the physical system the governing equations describe, form upon normalization dimensionless coefficients of the terms having unit order. These coefficients, or dimensionless parameters then, give an indication as to the importance of each of the terms in the governing equations.

The variables in normalized form become:

$t' = t/t_c$ - time coordinate

$x' = x/x_c$ - axial space coordinate

$y' = y/y_c$ - transverse (normal) space coordinate

$p' = \frac{p - p_e}{p_c}$ - pressure

$u' = u/u_c$ - axial velocity

$v' = \frac{v}{v_c}$ - transverse velocity

$\theta_L' = \frac{T_L - T_f}{T_o - T_f}$ - liquid temperature

$\theta_s' = \frac{T_s - T_f}{T_w - T_f}$ - solid temperature

Where: p_e =the fluid pressure at the freezing section outlet

T_o = inlet fluid temperature

T_f = fusion temperature of the liquid

T_w = the wall temperature of the cooled plate

The superscript "$'$", designating a dimensionless variable of unit order of magnitude, while the subscript "c", indicates a characteristic quantity which is to be determined.

Using these quantities the continuity equation 2.1 - 1 becomes

$$\frac{\partial u'}{\partial x'} + \frac{x_c v_c}{y_c u_c} \cdot \frac{\partial v'}{\partial y'} = 0$$

Since the axial and transverse velocity gradients are of the same magnitude then

$$\frac{x_c v_c}{y_c u_c} \approx 1 \qquad 2.2 - 1$$

Substitution of the variables into the momentum and energy equations (2.1 - 2 through 2.1 - 5) leads to the following equations.

Momentum Equation - x component

$$\left[\frac{x_c}{u_c t_c}\right] \cdot \frac{\partial u'}{\partial t'} + u' \cdot \frac{\partial u'}{\partial x'} + \left[\frac{x_c v_c}{y_c u_c}\right] v' \cdot \frac{\partial u'}{\partial y'}$$

$$= - \left[\frac{p_c}{\rho_L u_c^2}\right] \cdot \frac{\partial p'}{\partial x'} + \left[\frac{\upsilon}{u_c x_c}\right] \cdot \frac{\partial^2 u'}{\partial x'^2} = \left[\frac{\upsilon x_c}{u_c y_c^2}\right] \cdot \frac{\partial^2 u'}{\partial y_c'^2} - \left[\frac{x_c}{u_c^2}\right] \cdot g_x$$

Momentum Equation - y component

$$\left[\frac{x_c}{u_c t_c}\right] \cdot \frac{\partial v'}{\partial t} + u' \cdot \frac{\partial v'}{\partial x} + \left[\frac{x_c v_c}{y_c u_c}\right] \cdot v' \cdot \frac{\partial v}{\partial y} = - \left[\frac{p_c}{\rho_L u_c v_c y_c}\right] \cdot \frac{\partial p'}{\partial y'}$$

$$+ \left[\frac{\upsilon}{u_c x_c}\right] \cdot \frac{\partial^2 v'}{\partial x'^2} + \left[\frac{\upsilon x_c}{u_c y_c^2}\right] \cdot \frac{\partial^2 v'}{\partial y'^2}$$

Energy Equation - liquid region

$$\left[\frac{x_c}{u_c t_c}\right] \cdot \frac{\partial \theta_L'}{\partial t'} + u' \cdot \frac{\partial \theta_L'}{\partial x'} + \left[\frac{x_c v_c}{y_c u_c}\right] \cdot v' \cdot \frac{\partial \theta_L'}{\partial y'} = \frac{\kappa_L}{\rho_L C_L} \left\{ \left[\frac{1}{u_c x_c}\right] \cdot \frac{\partial^2 \theta_L'}{\partial x'^2} \right.$$

$$\left. + \left[\frac{x_c}{u_c y_c}\right] \cdot \frac{\partial^2 \theta_L'}{\partial y'^2} \right\} + \frac{2\upsilon}{C_L} \left\{ \left[\frac{u_c}{(T_o - T_f)\, x_c}\right] \cdot \frac{\partial u'}{\partial x'}^{2} \right.$$

$$\left. + \left[\frac{u_c}{(T_o - T_f)\, x_c}\right] \cdot \left[\frac{x_c v_c}{y_c u_c}\right]^2 \cdot \left[\frac{\partial v'}{\partial y'}\right]^2 \right\} + \frac{\upsilon}{C_L} \left\{ \left[\frac{u_c}{(T_o - T_f)\, x_c}\right] \left(\frac{x_c}{y_c}\right)^2 \cdot \right.$$

$$\left(\frac{\partial u'}{\partial y'}\right)^2 + 2 \left[\frac{u_c}{(T_o - T_f)\, x_c}\right] \cdot \left[\frac{x_c v_c}{y_c u_c}\right] \cdot \frac{\partial u'}{\partial y'} \cdot \frac{\partial v'}{\partial x'}$$

$$\left. + \left[\frac{u_c}{(T_o - T_f)\, x_c}\right] \cdot \left(\frac{v_c}{u_c}\right)^2 \cdot \left(\frac{\partial v'}{\partial x'}\right)^2 \right\}$$

Energy Equation - solid region

$$\frac{\rho_s C_s}{\kappa_s} \left[\frac{y_c^2}{t_c}\right] \cdot \frac{\partial \theta_s'}{\partial t'} = \left[\frac{y_c}{x_c}\right]^2 \cdot \frac{\partial^2 \theta_s'}{\partial x'^2} + \frac{\partial^2 \theta_s'}{\partial y'^2}$$

The governing equations are written in the above form as it is expected that in the liquid region the convection and advection terms will be important, and hence of order unity. For the energy equation in the solid the normal temperature gradient is a dominant term if growth of a solid phase is to occur.

A suitable characteristic quantity for y_c in the solid region would be the steady state (fully developed) solid thickness. If this value is teemed s_f, the time scale t_c may be determined from the energy equation of the solid by noting that the transient is of the same order as the transverse conduction only if:

$$\frac{\rho_s C_s}{k_s}\left[\frac{s_f^{\,2}}{t_c}\right] \simeq 1$$

Hence $$t_c = \frac{\rho_s C_s \; s_f^{\,2}}{k_s} = \frac{s_f^{\,2}}{\alpha_s} \qquad 2.2 - 2$$

The time scale could have been determined from the governing equations for the liquid region. It, however, would have involved determination of additional characteristic quantities. It should be noted that the above definition gives the rate of solidification of the solid phase directly in terms of the properties of the solid.

Examination of the foregoing equations reveals that after some manipulation the following dimensionless groupings may be made to appear:

$\alpha = \dfrac{\alpha_L}{\alpha_s}$, the thermal diffusivity ratio

$Re_c = \dfrac{u_c y_c}{\upsilon}$, the characteristic Reynold's number

$Pr = \dfrac{\upsilon}{\alpha_L}$, the Prandtl number

$Pe = Re_c \cdot Pr$, the Péclèt number

$Fr = \frac{u_c{}^2}{y_c g}$, the Froude number

$Eu = \frac{P_c}{\rho_L u_c{}^2}$, the Euler number

$\delta = \frac{y_c}{x_c}$, scale factor liquid region

$\delta_s = \frac{s_f}{x_c}$, scale factor solid regions

The governing equations become:

Momentum equation - x component

$$\frac{1}{\delta \alpha P_e} \cdot \left[\frac{y_c^2}{\alpha_s t_c}\right] \cdot \frac{\partial u'}{\partial t'} + u' \cdot \frac{\partial u'}{\partial x'} + v' \cdot \frac{\partial u'}{\partial y'} = -Eu \cdot \frac{\partial p'}{\partial x'}$$

$$+ \frac{1}{\delta Re_c} \left[\delta^2 \frac{\partial^2 u'}{\partial x'^2} + \frac{\partial^2 u'}{\partial y'^2} \right] - \frac{1}{\delta Fr} \cdot \frac{g_x}{g} \qquad 2.2 - 3$$

Momentum equation - y component

$$\frac{1}{\delta \alpha P_e} \left[\frac{y_c{}^2}{\alpha_s t_c}\right] \cdot \frac{\partial v'}{\partial t'} + u' \cdot \frac{\partial v'}{\partial x'} + v' \cdot \frac{\partial v'}{\partial y'} = - \frac{Eu}{\delta^2} \cdot \frac{\partial p'}{\partial y'}$$

$$+ \frac{1}{\delta\ Re_c} \cdot \left[\delta^2 \frac{\partial^2 v'}{\partial x'^2} + \frac{\partial^2 v'}{\partial y'^2} \right] \qquad 2.2 - 4$$

Energy equation - liquid phase

$$\frac{1}{\delta \alpha P_e} \cdot \left[\frac{y_c{}^2}{\alpha_s t_c} \right] \cdot \frac{\partial \theta_L'}{\partial t'} + u' \cdot \frac{\partial \theta_L'}{\partial x'} + v' \cdot \frac{\partial \theta_L'}{\partial y'} =$$

$$\frac{1}{\delta P_e} \cdot \left[\delta^2 \frac{\partial^2 \theta_L'}{\partial x'^2} + \frac{\partial^2 \theta_L}{\partial y'^2} \right] + \frac{E}{\delta Re_c} \cdot \Phi$$

Where

$$\Phi = \left[\frac{\partial u'}{\partial y'} + \delta^2 \frac{\partial v'}{\partial x'} \right]^2 + 2\delta^2 \left\{ \left[\frac{\partial u'}{\partial x'} \right]^2 + \left[\frac{\partial v'}{\partial y'} \right]^2 \right\} \qquad 2.2 - 5$$

is the dissipation function.

Energy Equation - solid phase

$$\frac{\partial \theta_s'}{\partial t'} = \delta_s \frac{\partial^2 \theta_s'}{\partial x'^2} + \frac{\partial^2 \theta_s'}{\partial y'^2}$$

Axial conduction in the solid phase in comparison with conduction in the transverse direction is negligible provided $\delta_s \ll 1$. Similarly in the liquid phase axial conduction can be ignored in relation to the transverse conduction term if $\delta \ll 1$. Comparison between the advection term and the dissipation term shows that for $\frac{E}{Re} \ll \delta$, viscous dissipation can be neglected. The value of δ used, moreover, depends on the choice of the characteristic quantities y_c and x_c. Like the classical boundary layer problems this choice depends upon the region of interest. Near the entrance of the freezing zone $x \longrightarrow 0$ so that a suitable value for y_c might be the boundary layer thickness, while for regions farther downstream the choice could be the fully developed fluid thickness.

In a fashion similar to the energy equations, examinations of the x - component of momentum reveals that the viscous force term $\frac{\partial^2 u'}{\partial y^2}$, is small when compared with the viscous force term represented by $\frac{\partial^2 u'}{\partial y^2}$ provided $\delta \ll 1$. Moreover, if $Re_c \gg 1 \gg \delta$, the magnitude of both viscous forces would be negligible, though the term $\frac{\partial^2 u'}{\partial y^2}$ would still have to be retained in order to satisy the transverse boundary conditions. As the flow is assumed vertical the only body force which occurs is in the axial direction. It may be disregarded provided $\frac{1}{Fr} \ll \delta$. Experimentally, with the low velocities which would be

incurred, this condition did not prevail. The driving force, $\frac{\partial p'}{\partial x'}$, was naturally also retained, implying Eu ≃ 1 from which the scale factor for the pressure is found to be : $p_c \simeq \rho_L u_c^2$. The y - component of the momentum equation reduces to $\frac{\partial p'}{\partial y'} = 0$ provided $\frac{\delta}{Re_c} << 1$.

2.3 Mathematical Model

Based on the results of the previous section it is advantageous to introduce the following set of dimmensionless variables.

$\tau = \frac{\alpha_s t}{d^2}$ dimensionless time coordinate

$\eta = \frac{y_i}{d}$ dimensionless thickness of the liquid

$X = \frac{x}{\ell}$ dimensionless axial coordinate

$Y = \frac{y}{d}$ dimensionless transverse coordinate

$P = \frac{p - p_e}{\rho Um^2}$ dimensionless pressure

$U = \frac{u}{Um}$ dimensionless axial velocity

$V = \frac{v\ell}{dUm}$ dimensionless transverse velocity

$\theta_L = \frac{T_L - T_f}{T_o - T_f}$ dimensionless liquid phase temperature

$\theta_S = \frac{T_s - T_f}{T_f - T_w}$ dimensionless solid phase temperature

Where d = the distance between the parallel plates

Um = the average velocity at time $t = 0$.

The mathematical formulation defined by the simplified governing equations, initial and boundary conditions becomes:

Continuity Equation

$$\frac{\partial U}{\partial x} + \frac{\partial V}{\partial y} = 0 \qquad 2.3 - 1$$

Momentum Equation

X - component

$$\frac{1}{\delta\alpha P_e}\frac{\partial U}{\partial \tau} + U\frac{\partial U}{\partial X} + V\frac{\partial U}{\partial Y} = -\frac{\partial P}{\partial X} + \frac{1}{\delta R_e}\frac{\partial^2 U}{\partial Y^2} + \frac{1}{\delta F_r} \qquad 2.3 - 2$$

Y - component

$$0 = -\frac{\partial P}{\partial Y}$$

Energy Equation

Liquid Phase

$$\frac{1}{\delta\alpha P_e}\frac{\partial \theta_L}{\partial \tau} + U\frac{\partial \theta_L}{\partial X} + V\frac{\partial \theta_L}{\partial Y} = \frac{1}{\delta P_e}\frac{\partial^2 \theta_L}{\partial Y^2} \qquad 2.3 - 3$$

Solid Phase

$$\frac{\partial \theta_s}{\partial \tau} = \frac{\partial^2 \theta_s}{\partial Y^2} \qquad 2.3 - 4$$

Initial Conditions @ $\tau = 0, \quad 0 \leqslant Y \leqslant 1, \quad 0 \leqslant X \leqslant 1$

$$U(X, Y, 0) = 6(Y - Y^2)$$

$$V(X, Y, 0) = 0 \qquad 2.3 - 5$$

$$\theta_L(X, Y, 0) = 1$$

$$\theta_s(X, Y, \tau = 0^+) = 0$$

Inlet Boundary Condition @ $X = 0, \; 0 \leqslant Y \leqslant 1, \quad \tau > 0$

$$\frac{1}{\delta\alpha P_e}\frac{\partial U}{\partial \tau} = -\frac{\partial P(x, \tau)}{\partial X} + \frac{1}{\delta R_e}\frac{\partial^2 U}{\partial Y^2} + \frac{1}{\delta Fr} \qquad 2.3 - 6$$

With the above initial conditions and the following conditions,

$$U(0, 0, \tau) = 0$$

$$U(0, 1, \tau) = 0$$

Wall Boundary Conditions

$$@\ Y = 0,\ 0 \leqslant X \leqslant 1, \qquad U(X, 0, \tau) = V(X, 0, \tau) = 0 \qquad 2.3\text{-}7$$

$$\frac{\partial \theta_L}{\partial Y}(X, 0, \tau) = 0$$

$$@\ Y = 1,\ 0 < X \leqslant 1, \qquad \theta_s(X > 0, 1, \tau) = \theta_w = \text{constant}$$

Interface Boundary Conditions

$$@\ Y = \eta,\ 0 < X \leqslant 1,\quad \tau < 0$$

$$U(X, \eta, \tau) = V(X, \eta, \tau) = 0$$

$$\theta_L(X, \eta, \tau) = \theta_s(X, \eta, \tau) = 0 \qquad 2.3 - 8$$

$$\left.\frac{\partial \theta_s}{\partial Y}\right|_{Y=\eta} \cdot \sigma = \kappa \cdot \left.\frac{\partial \theta_L}{\partial Y}\right|_{Y=\eta} + \frac{1}{Ste}\frac{d\eta}{d\tau}$$

Examination of the above reveals the following dimensionless parameters.

$\delta = \frac{d}{\ell}$ scale factor

$\alpha = \frac{\alpha_L}{\alpha_s}$ thermal diffusivity ratio

$Re = \frac{Umd}{\nu}$ Reynolds number

$Pe = \frac{Umd}{\alpha_L}$ Péclèt number

$\kappa = \frac{\kappa_L}{\kappa_s}$ ratio of thermal conductivities

$\sigma = \frac{T_f - T_w}{T_o - T_f}$ superheat ratio

$Ste = \frac{C_s(T_o - T_f)}{L}$ Stefan number; ratio of liquid sensible heat to the latent heat

$Fr = \frac{Um^2}{dg}$ Froude number

In order to ensure that the velocity profiles obtained from the momentum equation 2.3 - 2 are valid, the pressure gradient term must satisfy the integral continuity equation.

$$\int_0^1 UdY - \int_0^\eta UdY = \frac{1 - \rho}{\delta\alpha P} \int_0^X \frac{\partial\eta}{\partial\tau} dx \qquad 2.3 - 9$$

The equation is derived in Appendex A by considering a control volume surrounding part of the freezing section. The first term representing the axial mass influx at X = 0, while the second term is the axial mass efflux at some distance X. The difference in these terms is the mass flow at the liquid - solid interface.

2.4 Assumptions

The assumptions used in the derivation of the mathematical model represented in section 2.3 may be summarized as:

1. The liquid flow is assumed to remain laminar and two dimensional throughout the freezing section.
2. The liquid is assumed to be Newtonian possessing constant viscosity.
3. Both the solid and liquid phases have constant density, constant thermal conductivity, and constant diffusivity.
4. The temperature of the cooled wall is assumed constant and below the freezing point of the liquid, whereas the opposing wall is assumed to be adiabatic.
5. Axial conduction in both phases is negligible.

6. In the liquid phase the viscous force due to the axial shear, dissipation and transverse pressure gradient are neglected.
7. The velocity profile of the liquid at the entrance to the freezing section is fully developed but not invariant.
8. The liquid temperature at the inlet of the freezing section is constant.
9. The pressure drop across the system is constant.

CHAPTER III

EXPERIMENTAL INVESTIGATION

3.1 Requirements

It was intended that the experimental data obtained be representative enough so that a comparison with any analytical study of the model proposed in Chapter II could be made. The apparatus, moreover, was to be sufficiently flexible that other conditions could be investigated, in particular the effect of turbulence and natural convection. The chief concern of any study involving a moving liquid undergoing a solidification or melting process is the amount and rate at which the phase change occurs and the effect on the system pressure drop. This imposes the obvious difficulty of determining the location of the liquid-solid interface without disturbing the flow.

The experimental design as a physical realization of a mathematical model can only hope to approach the conditions the model prescribes. It must, nevertheless, accurately produce the assumptions imposed by the theoretical analysis if a comparison is to have validity. This implies that several constraints be applied to the experimental design and testing procedure:

1. Since the test section must have a finite width, any channel chosen would have an aspect ratio, γ, which approached zero.
2. The hydrodynamic entrance length was to be sufficient to produce a fully developed velocity profile at the inlet to the freezing zone for all laminar flow conditions.
3. Boundary layer formation on the side walls was to be negligible.
4. The surface roughness, waviness, discontinuities, and section variances were to be minimized as best as possible.

5. Axial conduction resulting from the step temperature change was to be minimized.
6. The growth of the solidified layer was to be of sufficient thickness to obtain accurate results.
7. The material for the insulated walls was to be a poor enough heat conductor to eliminate ambient heat conduction effects.
8. None of the dimensionless parameters should violate any of the assumptions posed by the order of magnitude analysis.
9. The total system pressure drop should not vary appreciably during a test.

In addition, it was felt desirable to observe the solid layer during the transient conditions. This necessitated the side walls, at least, to be constructed of an optically transparent material. Although some of the above requirements appear to conflict, an adequate design can still be properly constructed.

3.2 Description of Experimental Apparatus

The apparatus was considered to consist of two separate systems; the "coolant" system which determined the boundary condition on the cooled wall of the freezing zone and the "warm water" system which provided the internal flow between plates. A schematic of the apparatus is shown in figure 3.1, photographs of the system in figure 3.2 and 3.3, while construction drawings are given in Appendix B. A list of manufacturers of the various equipment used is given in Appendix C.

The coolant system was a closed loop consisting primarily of a reservoir, pump, control valve, flexible piping and test section cooling jacket. The coolant fluid, a water-ethylene glycol mixture,

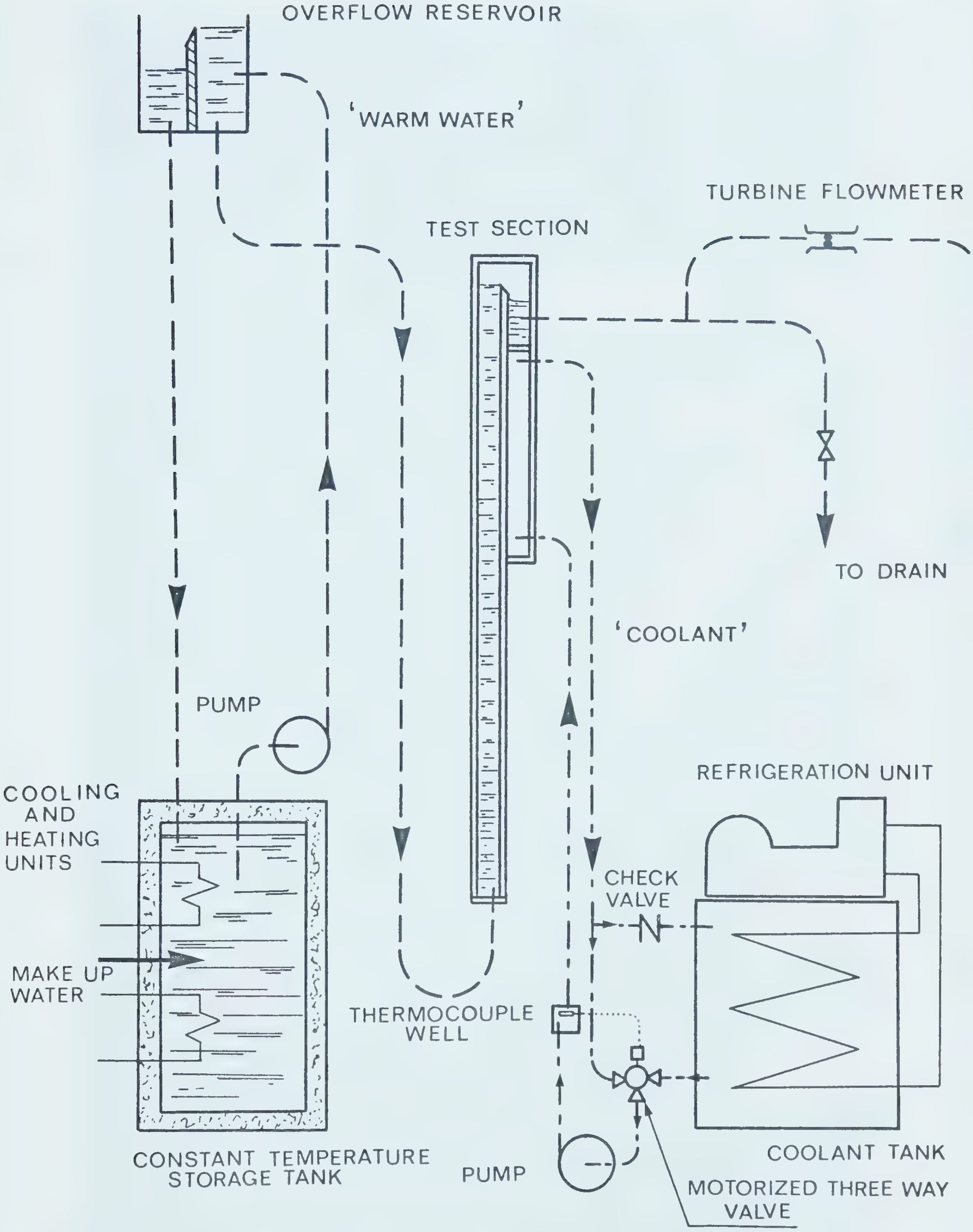

FIGURE 3.1 SCHEMATIC OF EXPERIMENTAL APPARATUS

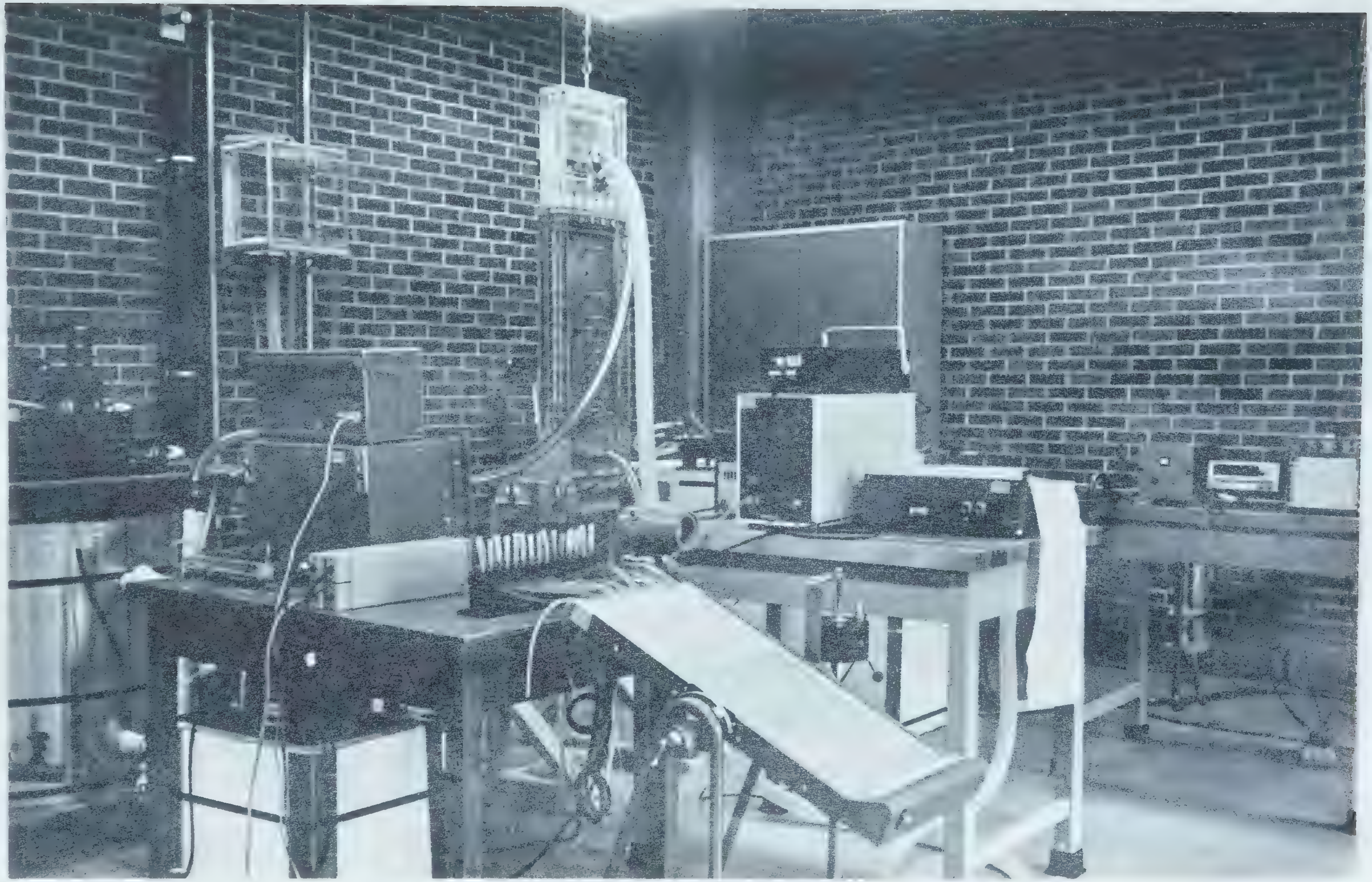

FIGURE 3.2 EXPERIMENTAL APPARATUS

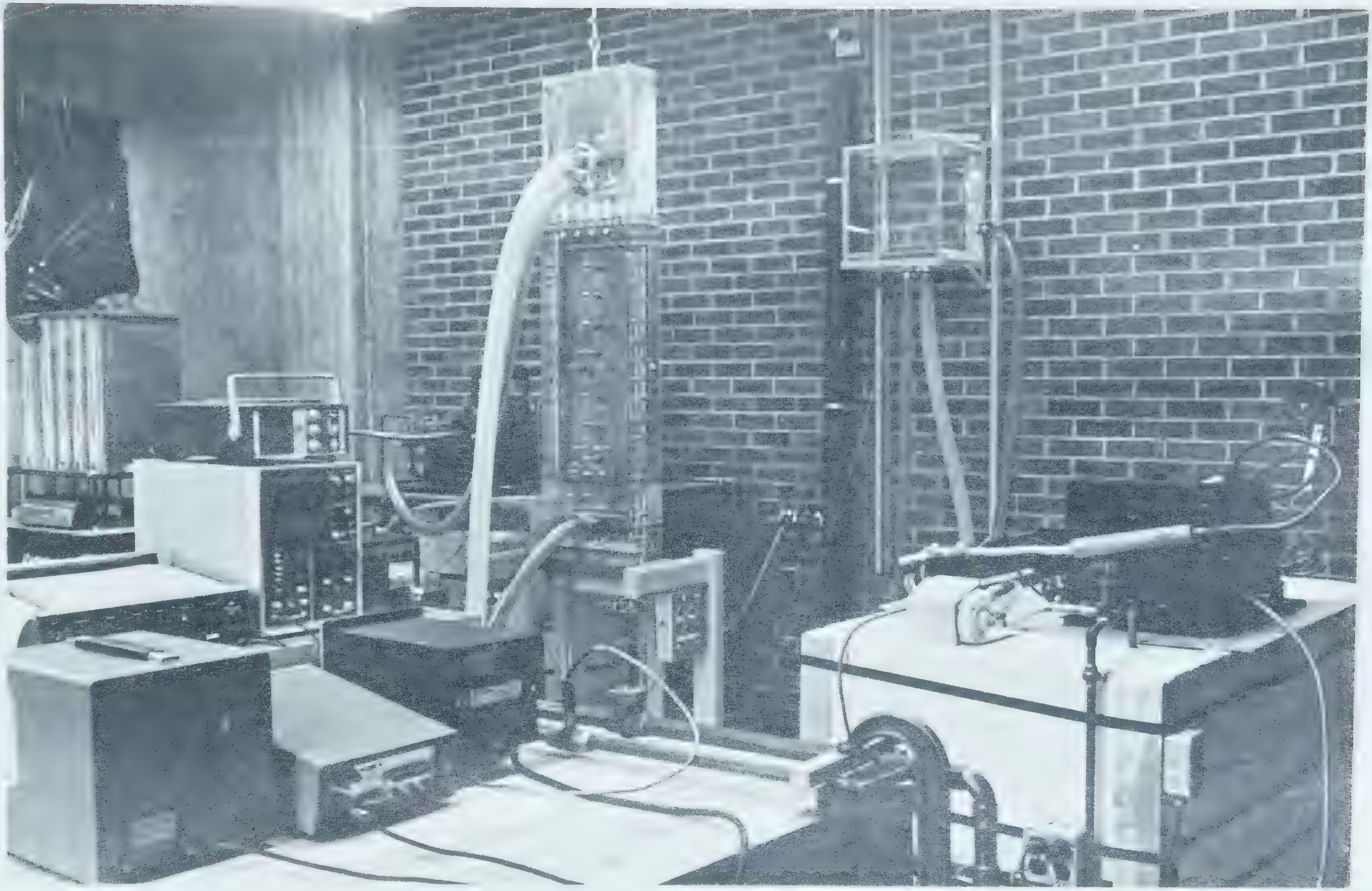

FIGURE 3.3 EXPERIMENTAL APPARATUS

was pumped through the cooling jacket where it gained heat transferred from the "warm water" side of the freezing section. The coolant's temperature was maintained by means of a temperature controlled three way valve which mixed recirculated coolant with refrigerated coolant from the reservoir.

The "warm water" system was an open loop where water at a constant temperature was pumped from a temperature controlled storage tank to an overflow reservoir. Excess water from the reservoir spilled back to the storage tank while the remaining water flowed to the test section. This water was then forced upwards between two insulating parallel plates allowing the velocity profile to become fully developed before entering the freezing zone. As it passed through the freezing section the water cooled and some of it solidified forming an ice layer on the cooled wall. The cooled water continued to the upper reservoir where it spilled over a weir and flowed down into a turbine flowmeter from which it finally was discharged into a drain. Since gravity acted as the driving force, the total head acting on the system was dependent on the height differential between the top of the weirs in the overflow and upper reservoirs. Thus the initial flow rate was varied by raising or lowering the overflow reservoir.

3.2.1. Test Section

The test section or freezing zone consisted primarily of two rectangular channels separated by a heat conducting wall. A simplified cross sectional view is shown in figure 3.4. A photograph of the "warm water" side may be seen in figure 3.5 while the "coolant" side is shown in figure 3.6. For a more detailed description the reader should refer

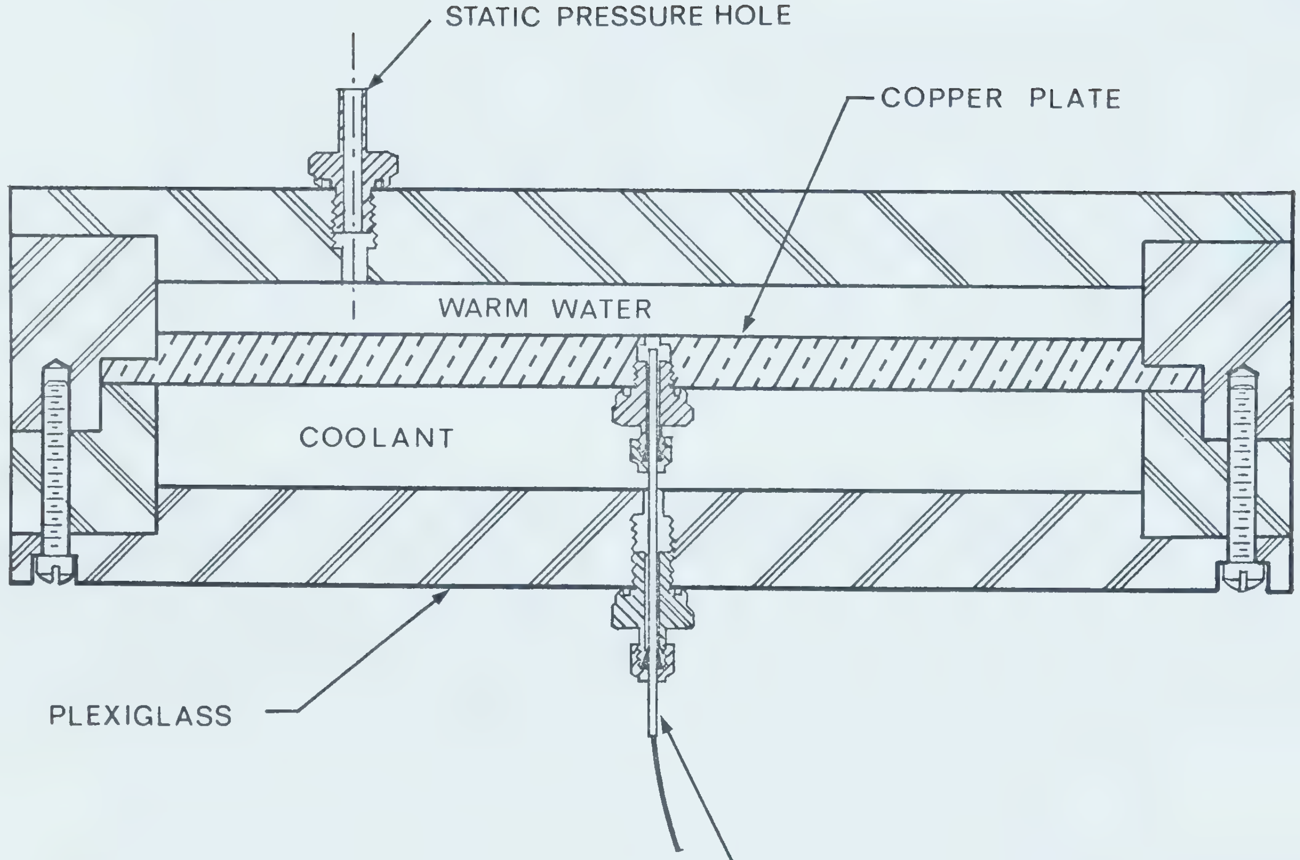

FIGURE 3.4 TEST SECTION – CROSS SECTIONAL VIEW

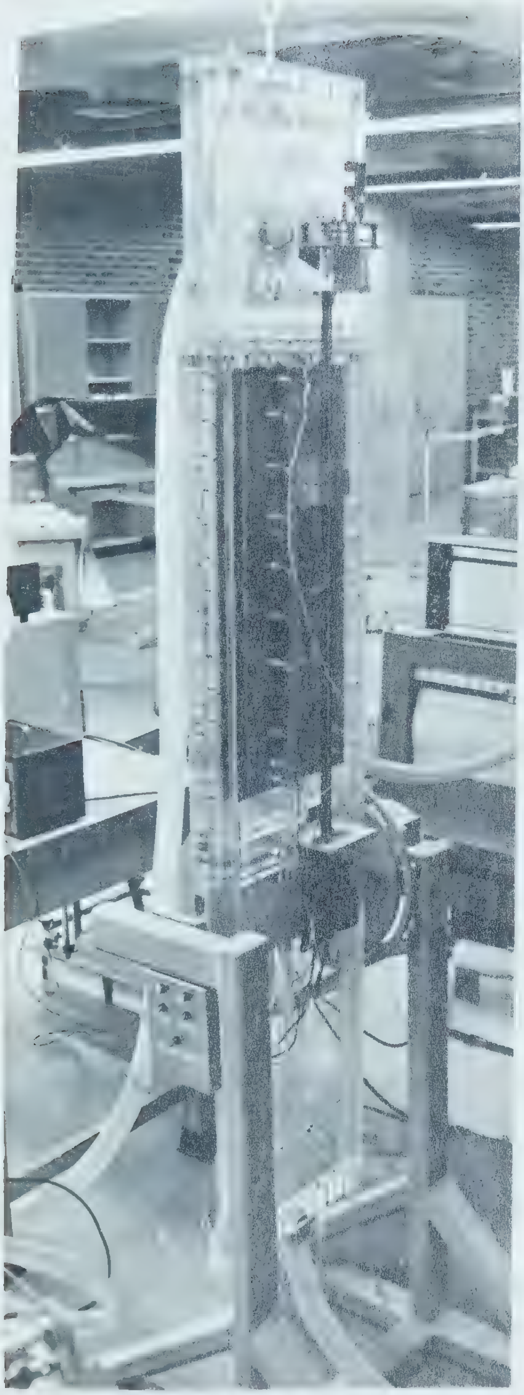

FIGURE 3.5 WARM WATER SIDE

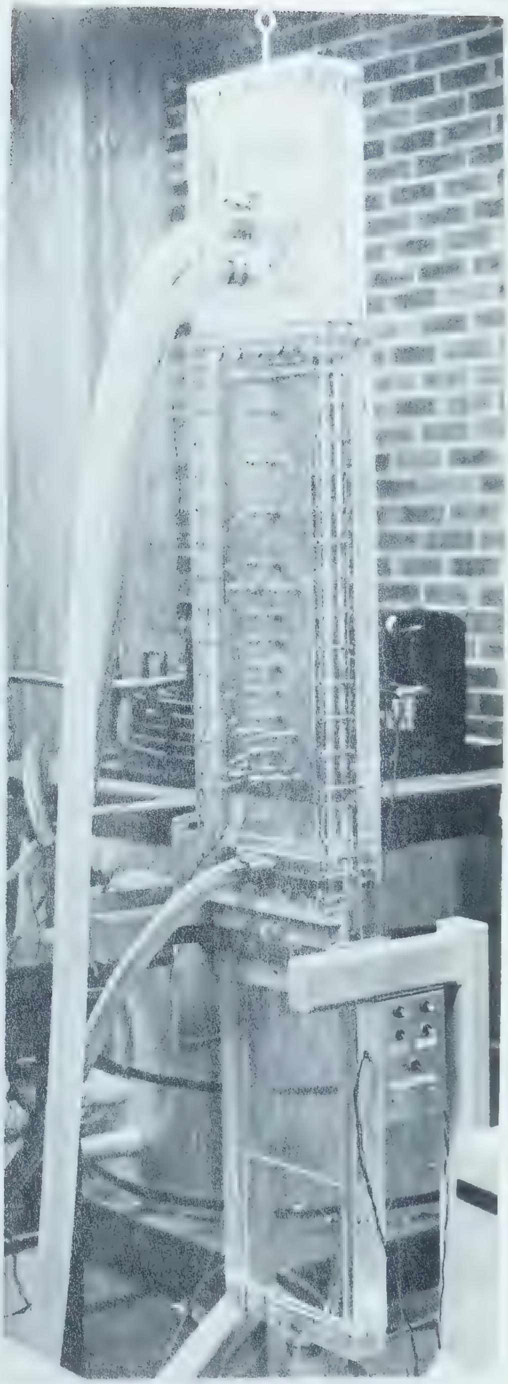

FIGURE 3.5 COOLANT SIDE

to Appendix B, DWG B1 to DWG B4.

The dividing wall was ½ inch thick copper plate which provided a freezing length, l, of 24 inches and a freezing wide, b, of 10 inches. Copper was chosen because of its high thermal conductivity, low heat capacity. The plate was clamped between channels constructed from 1 inch and 1½ inch thick plexiglass. Plexiglass was chosen as it provided good visibility and insulation properties. Leakage between the "warm water" and "coolant" sides was prevented by use of 1/8 inch O-rings, and by chloroform welding of the plexiglass channel joints.

The distance, d, between the plexiglass and the copper plate on the "warm water" side was set at ½ inch, which gave an aspect ratio, γ, of 0.05. Rudimentary calculations indicated that with this aspect ratio, the effect of boundary layer growth on the side walls could be ignored for all but the lowest Reynold's numbers.

To ensure efficient heat transfer from the coolant, flow in the coolant channel should be turbulent. Due, however, to the high viscosity of the coolant at temperatures in the operating range - 30°F to 10 ° F, and also due to a limited pump capacity; the coolant flow could not be made turbulent without resorting to very small gap sizes. Instead the depth of the coolant channel was made 1 inch to suit space limitations required by the thermocouple probes. Provision was made for vortex generators in the form of triangular plexiglass blocks to be cemented in a staggered pattern to the plexiglass wall. Since the inlet flow to the coolant channel was turbulent (because of the small diameter of the inlet piping), the generators acted merely to sustain the turbulent flow.

3.2.2. Adiabatic Section

The section was in essence a continuation of the "warm water" side of the test section except that it was completely constructed of plexiglass. The upper 1½ inch thick plexiglass plate was continuous the length of the apparatus, while the lower plate was shorter butting against the copper plate of the freezing section. A smooth transition was made from the plexiglass to the copper plate.

The adiabatic section provided the entry length required to ensure the velocity profile entering the freezing section was fully developed. From the study done by Han [35] the entry length required was calculated to be 28.6 inches. The section, however, was constructed with a 32 inch length. Dye injected into the fluid stream as a check showed that the velocity profiles were in fact fully developed at the entrance to the freezing zone.

3.2.3. Lower and Upper Reservoirs

The purpose of these reservoirs was to mainly provide means of supplying and discharging fluid from the test section. The lower reservoir acted as a diffusing section for the fluid entering the adiabatic section. This was useful as it reduced the head loss that would have been caused by a sudden area cross section enlargement. The upper reservoir served as the discharge point for both the "warm water" and the "coolant" system. A weir 8 inches in height was used as the discharge point for the "warm water" system.

The reservoirs were entirely constructed of plexiglass except for the piping connections. Joints were welded by chloroform as in other portions of the apparatus; 1/8 inch O-rings provided the necessary seals. The construction drawing of the upper reservoir is given in DWG - B5

while the lower reservoir in DWG - B6, both in Appendix B.

3.2.4. Overflow Reservoir

The overflow reservoir consisted of a rectangular plexiglass tank mounted on a carriage constructed from 1 inch angle iron. The carriage utilized ball bearing wheels which were constrained to move vertically by two 7 foot 6 inch channels bent from 16 gauge galvanized sheet metal. A pulley system consisting of a pair of pulleys, windlass and steel wire strand was used to raise or lower the reservoir and carriage.

The reservoir itself was composed of two compartments separated by a weir 14 inches in height. "Warm water" was pumped rapidly enough from the storage tank to fill the first compartment. Some of this incoming water was discharged from a pipe connection at the base of the compartment and flowed towards the test section. The rest of the water spilled over the weir into the second compartment where upon it was returned to the storage tank.

3.2.5. Apparatus Support Stand

The adiabatic and freezing sections were supported by a stand constructed from 3 inch by 2 inch rectangular tubing. The sections were bolted to a mounting plate which in turn was bolted to an axle. The axle was supported by two roller bearings mounted onto two arms of the stand. A gearbox keyed onto the axle shaft allowed the test section to be rotated to any angle 0° to 90° off the vertical. This was accomplished by turning a hand crank on the gearbox. A counterweight system was used to reduce the loading on the worm-gear drive. Although the gear ratio was high enough so that no additional braking was necessary, a locking mechanism was added to eliminate chance movement. A simple needle

pointer arm, screwed to the centreline of the axle and extending over the protracted range, indicated the amount of inclination of the apparatus.

Prior to testing the stand was levelled and bolted to the laboratory floor. The gearbox, pointer and locking mechanism can be seen in figure 3.7. A photograph of the apparatus shown inclined is given in figure 3.8.

3.2.6. Instrumentation

The primary measurements recorded during the course of an experimental test would be:

1) the ice layer thickness throughout its transient growth and at its steady-state position
2) the surface temperature along the copper plate as a function of time
3) the bulk temperatures of both the coolant and water flowing the test section
4) the mass flow of the water as a function of time
5) the pressure profile throughout the test section as a function of time

While most of the measurement techniques used were standard and call for little explanation, others may require a more detailed description.

Perhaps the most difficult instrumentation problem encountered with solidification studies involves the measurement of the solid phase thickness. Siegel and Savino [17] employed three techniques referred to as photographic, visual (utilizing a cathetometer and grid sheets), and

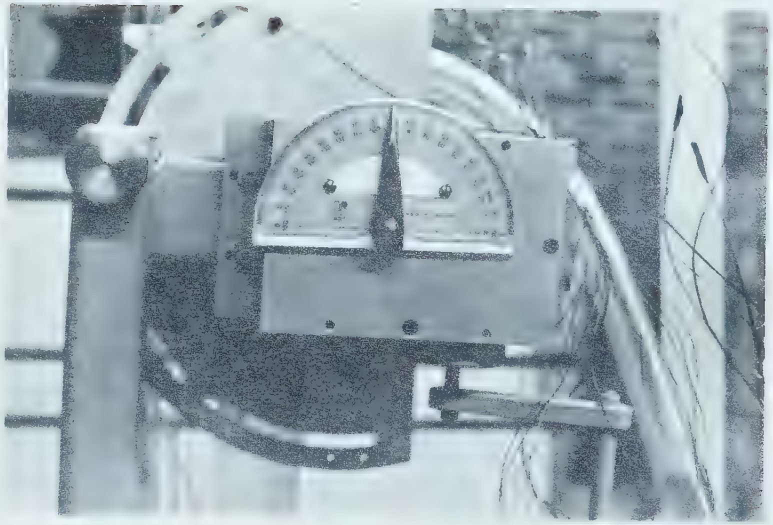

FIGURE 3.7 GEARBOX & POINTER

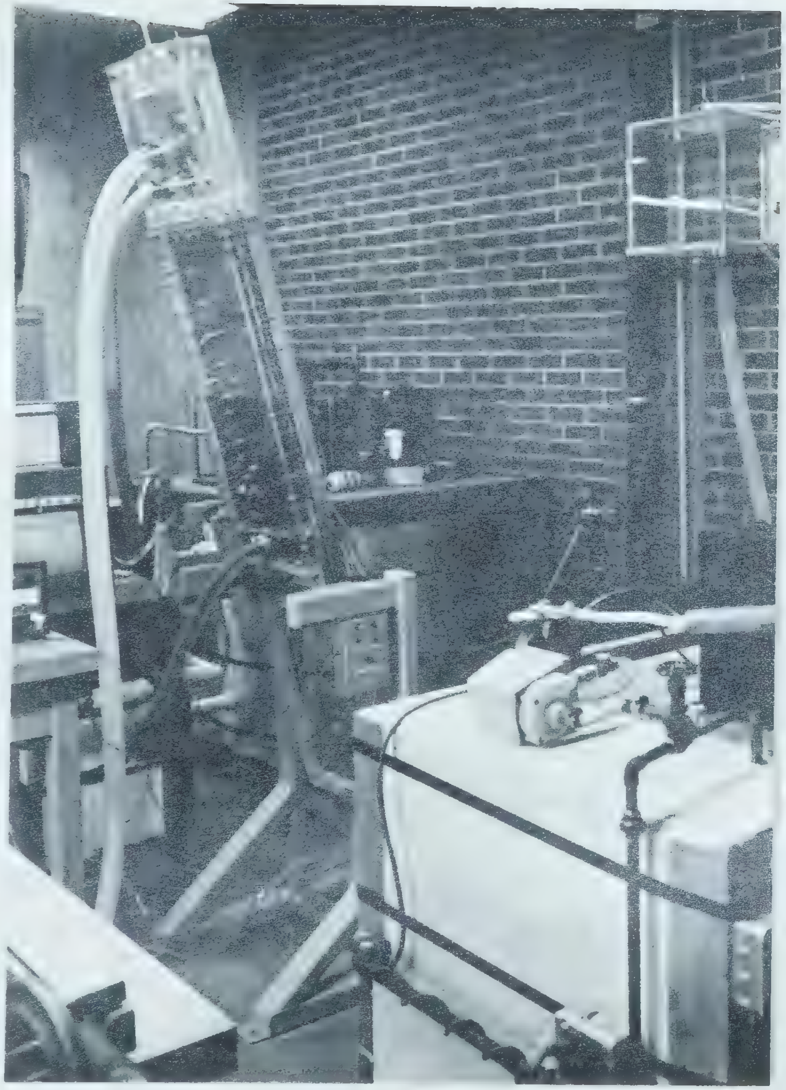

FIGURE 3.8 INCLINED TEST SECTION

temperature probe methods. Gort [21] developed a probe which deployed mechanical arms to detect the solid phase surface. Nyren [29] used a finger like sensing arm and voltage transducer to produce a continuous interface profile reading. Bailey and Dula [36] and Freeborn [26] demonstrated that ultrasonic signals can be made to accurately determine the water-ice interface without the inherent disadvantage, associated with mechanical probes, of disturbing the liquid phase.

Ultrasonics were adopted as the method seemed to provide the most feasible solution. Due to the narrow gap between the test section wall, any mechanical probe devised would have required a high degree of miniaturization. The problem, moreover, seemed ideally suited to the acoustical technique as copper has an exceptionally high reflectivity to sound waves. This enabled a clear distinction to be made between sound signals returning from the various interfaces.

The ultrasonic unit, a Branson "Sonoray 600", was operated in the pulse-echo mode using a single transmission-receiver transducer. The transducer probe would generate an initial pulse (usually referred to as the big bang). Reflections, or echos, would be received from each surface as shown by the typical pulse-echo signal depicted in figure 3.9. The time lag between the echos returned from the copper plate and the ice-water interface determined the thickness of the ice. Through the use of an electric timing gate, the Branson Time Analog Gate, an analog signal of the ice thickness was received. This signal corresponded to a precalibrated thickness.

The probe was held flat against the outer plexiglass surface of the test section by a carriage, as illustrated in figure 3.10. A lead screw connected to a reversing D. C. motor allowed the carriage to traverse

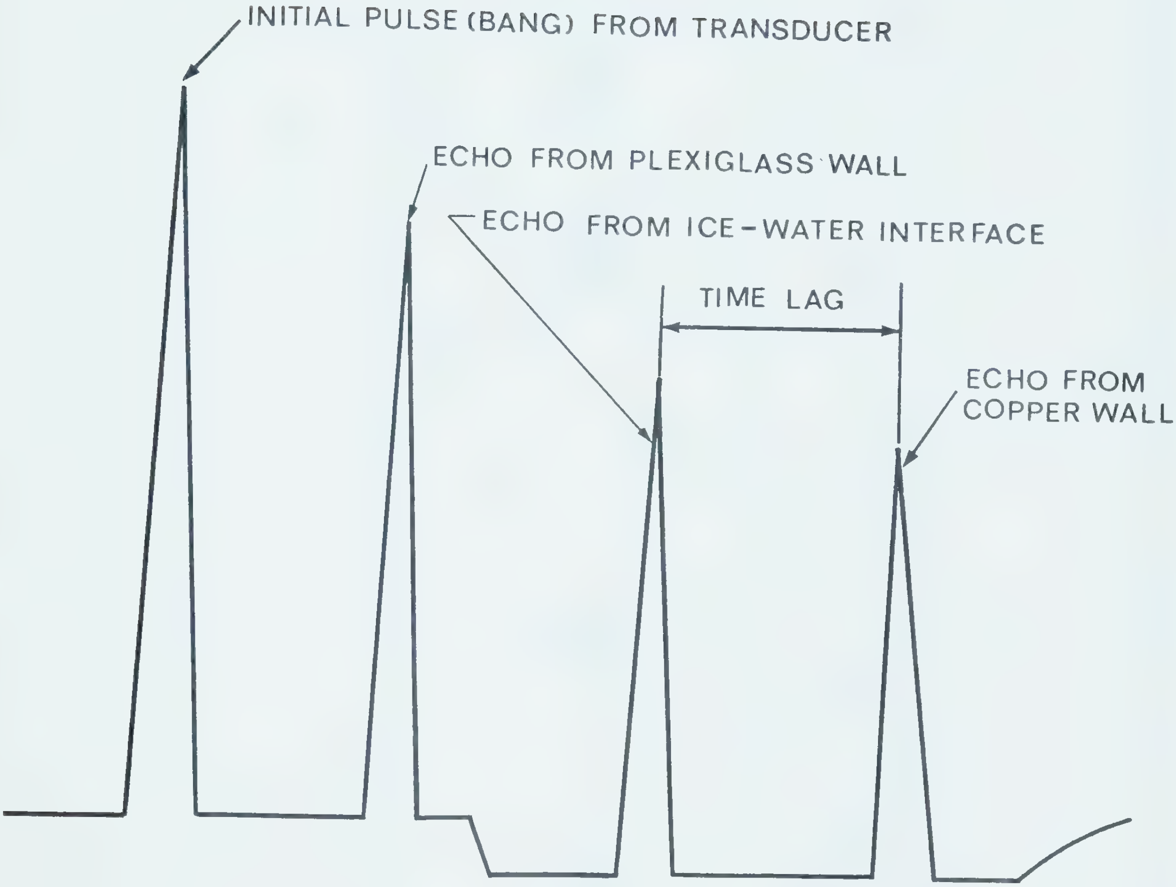

FIGURE 3.9 TYPICAL ULTRASONIC PULSE-ECHO SIGNAL

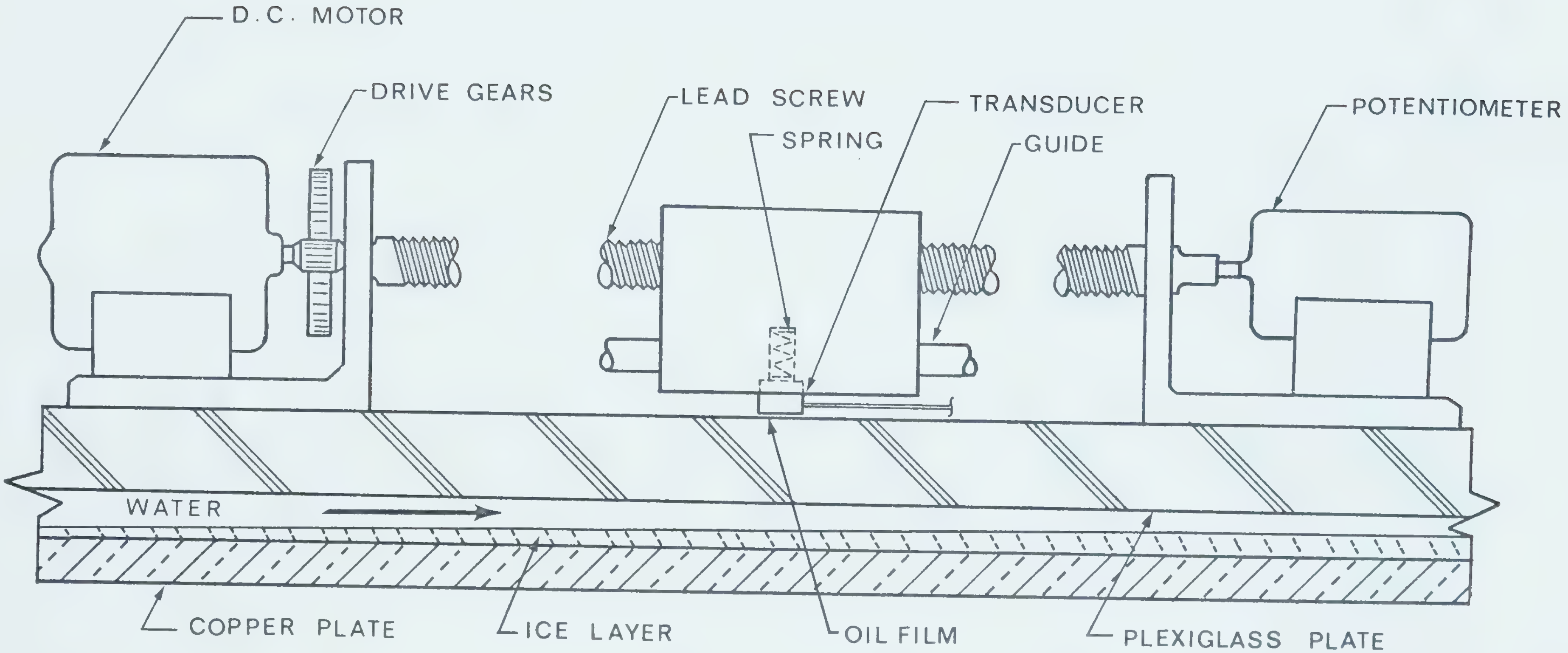

FIGURE 3.10 PROBE TRAVERSE MECHANISM

back and forth along the centreline of the test section. A thin film of oil was needed to act as a couplant between the transducer and plexiglass surfaces. A ten turn potentiometer monitored the position of the probe by varying the voltage from a fixed datum. Signals from the timing analog and the potentiometer were then used to drive a X-Y recorder. Thus a profile of the ice-water interface throughout any portion along the centreline of the test section could be generated. In addition, the time required to complete a traverse was variable, and depended either on the power given to the D. C. motor or the positions chosen for the limit switches. This proved to be a useful feature as higher solidification rates necessitated faster profile generation in order to record the transient growth. A photograph of the ultrasonic unit used is given in figure 3.11 – while the traversing unit is photographed in figure 3.12.

The surface temperatures of the copper plate were measured by a series of specially constructed thermocouple probes spaced throughout the length of the plate. The arrangement of the probes concentrated most of them along the centreline of the plate and near the leading edge where most of the transient effects occurred: see DWG - B1, Appendix B. A typical probe (DWG - B2) consisted of a pair of 36 gage copper-constantan wires soldered to a copper insert disk. A surface groove 0.010 inches deep, 0.010 inches wide and 0.125 inches in length was machined into the insert and the thermocouple wire passed through a 1/16 inches diameter stainless steel tubing and soldered to 28 gage thermocouple extension wire.

The purpose of the thermocouple probe design was to provide accurate surface temperature measurements, particularly during the transient

FIGURE 3.11
ULTRASONIC UNIT

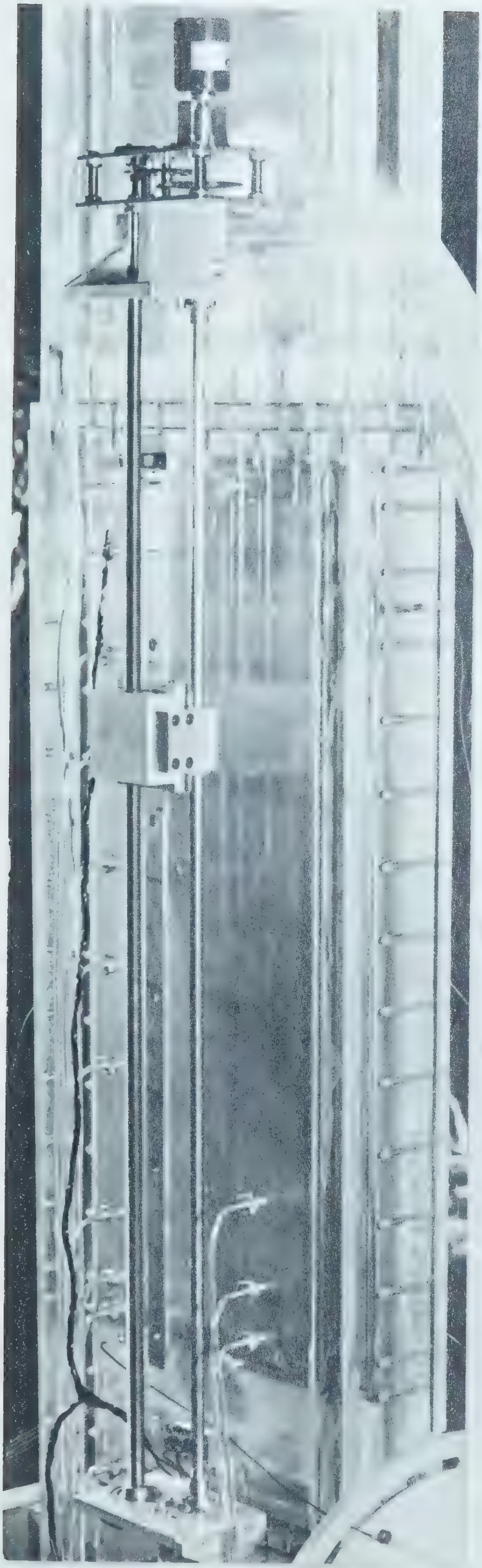

FIGURE 3.12 PROBE
TRAVERSE UNIT

conditions. The small diameter provided very rapid response times with a minimum of surface distortion. Initially attempts were made to fix the thermocouple wire directly to the copper plate. Due to the high heat conductivity of copper and the large surface area involved, soldering was not attempted. It was feared the amount of heat required would have induced excessive thermal distortion of the plate. Instead, surface grooves were machined into the plate and the thermocouple wires with their tips bared of insulation laid in place. The surrounding copper was then peened over the tips providing good thermocouple junctions. The wires were passed through holes drilled in the plate and the holes and remaining portion of the surface grooves filled with epoxy. Leakage, however, from the "coolant" to "warm water" side developed after a few preliminary runs. Due to the thermal expansion and the high fluid pressure on the "coolant" side, the epoxy was unable to adhere to the copper surface.

A particular advantage gained by the use of the redesigned thermocouples is that each thermocouple was a removable probe individually calibrated prior to installation (Chapter IV).

To determine the bulk temperatures of the fluids a standard immersion type probe was constructed. The probes were located at the inlets and outlets of the test section, and as well in the adiabatic section. Locations of the probes are given in Appendix B, DWG - B1.

The "warm water" system temperature was set and maintained by two thermostatically controlled 1500 watt immersion heaters installed in the constant temperature storage tank, or by a ½ ton refrigeration unit (figure 3.1). The temperature of the "coolant" system, however, was controlled by a resistance bulb thermometer located in the inlet line

to the test section. The thermometer produced a signal proportional to the desired temperature which activated a motor operated three-way control valve. This allowed previously cycled coolant to mix with the colder coolant from the reservoir. Specifications for both systems has been given in Appendix C.

The mass flow of the water flowing through the test section was obtained by use of a turbine flowmeter. The meter was located after the test section as there the pressure drop would not have any effect on the upstream conditions. A pickup generated an output frequency proportional to the flow rate. This signal was converted to a d. c. - milliampere output used to drive a continuous chart recorder. As the meter was accurate only between the range 0.8 - 8 g.p.m. an alternate collection system was used (by by-passing the turbine meter) if necessitated by the flow rate.

The pressure profile throughout the adiabatic and freezing zones was obtained by a series of static holes drilled along the outer plexiglass wall. The leads from these holes were connected to a multi-tube inclined mercury manometer. During the course of an experimental run a 35 - millimeter single reflex camera coupled with an automatic timer could photograph the manometer at predetermined time intervals to record the transient pressure variations. In addition to obtaining the pressure profile, two static holes were placed in line with the tops of the weirs in the upper and overflow reservoirs. Leads from these pressure taps were connected to a high sensitivity capacitance differential pressure transmitter.

CHAPTER IV

EXPERIMENTAL PROCEDURE

4.1 Calibration

Preliminary to actual testing the various instrumentation used by the apparatus required calibration. The Honeywell Electronik 15, low sensitivity twenty-four channel recorder was calibrated in conjuntion with the thermocouple probes prior to installation in the test section. The probes were immersed in a Rosemount Engineering Model 910AC calibration bath whose temperature was monitored by a Hewlett Packard quartz thermometer model 2801A, which had been previously calibrated against a platinum resistance thermometer. A calibration curve for each of the probes was determined for temperatures within the range of - 30 °F to 100°F. The factory calibration of the Brooks model 4901 - 10 turbine flowmeter was checked by collection of the water discharge. The Rosemount Engineering Model 1151 DP differential pressure transmitter was calibration against an inclined water manometer.

In order to obtain meaningful results from the ultrasonic thickness tester (Branson Instruments Sonoray 600) a means of calibration was developed. A small model duplicating the test section configuration was constructed and ice of a uniform thickness grown. The thickness of this "calibration" ice was measured by means of a micrometer probe similar to that developed by Siegel and Savino [17] . Essentially it consisted of a depth micrometer from which a thermocouple wire probe extended. The junction of the thermocouple was carefully lowered to the vicinity of the ice-water interface while the temperature response was noted. The position of the interface was considered determined

when the temperature reached the value of the freezing point. Using the ultrasonic tester the thickness was measured and adjusted to agree with the value obtained from the micrometer probe. The ultrasonic unit was now considered to be calibrated; various steel gauge blocks were measured and the results recorded. Thus as part of the experimental test procedure, the ultrasonic unit's calibration would be readily checked by again measuring the gauge blocks, and if necessary adjusting to reproduce the previously recorded results.

4.2 Test Procedure

The tests which can be conducted can be thought to be of two types, no-flow tests and flow tests. No-flow tests are performed to indicate the reproducibility of the results and to provide a comparison with studies available in literature. The procedure to be followed in conducting a flow test (a no-flow test having obvious deletions) would be as follows:

1. Water would be added to the constant temperature storage tank, and the temperature control set as desired.
2. The refrigeration unit would be turned on to cool down the coolant reservoir.
3. After a prolonged period, sufficient to allow for the escape of dissolved gases, and long enough for the water temperature to have stabilized, the "warm water" circulation pump would be started and the rate of flow to the overflow reservoir adjusted.
4. The elevation of the overflow reservoir would be adjusted by using the hand winch to give the desired pressure head as determined by the capacitance differential transmitter. If

necessary the flow rate from the "warm water" circulation pump would be again adjusted.

5. The turbine flowmeter pulse counter and chart recorder would be switched on, as would the multipoint temperature recorder.
6. The circulation pump would be switched off while the ultrasonic unit was calibrated by means of the gauge blocks.
7. The X-Y recorder would be switched on. The traversing unit's "cycle time adjusted and noted.
8. The ultrasonic transducer would be installed in the traversing unit.
9. All pressure taps to the manometer would be purged of air bubbles. The camera unit which was to record changes in the pressure distribution would be checked for focus and duration between pictures set.
10. The coolant temperature would be set.
11. The "warm water" circulation pump would be restarted.
12. After the flow and temperature had again stabilized, the coolant pump would be turned on.
13. The surface of the copper plate would be watched carefully. At the first appearance of an ice layer, $t = \tau = 0$, event markers would be manually tripped, and simultaneously the traversing unit and camera started.
14. A test would be terminated when either the ice layer approached complete flow blockage, the ice layer reached a steady-state condition, the motorized three way valve could no longer control the coolant inlet temperature, or the "warm water" reservoir was empted.

CHAPTER V

DISCUSSION

The study presented in this thesis is part of a long ranged investigation concerned with learning the effects caused by phase change in various flow configurations and flow conditions. Until very recently this field has received but scant attention. Eventually it is hoped that enough information will be obtained to enable the development of a flow control device to be designed based on the freezing process.

With this in mind the apparatus was designed to test more than the solution of the simplified mathematical model presented in Chapter II. The apparatus has been built to tilt so that the effects of natural convection could be looked into. The positive displacement "warm water" circulation pump could very simply be connected directly to the test section so that constant mass flow conditions could be studied. If the test section were to be inclined at or past the horizontal and the "warm water" flow rate controlled a three phase system; ice, water and air, could be studied-quantitatively at least. And of course the test section could be readily substituted for sections of various geometric configurations.

A few words should be mentioned about the preliminary testing of the system. Tests were run at various conditions to determine the type and quality of the ice. Since the accuracy of the ultrasonic measurement technique assumes that the "test" ice be similar to the ice grown for calibration purposes. Non-homogeneities and marked variations in the temperature gradient across the ice modify the velocity of sound creating an inherent error. In general the difference between the quality of the

"test" and "calibration" ice varied little. Additional checks were made by subtracting the measured thickness of the fluid stream (time lag between the plexiglass wall and the ice-water interface, (see figure 3.9) from the gap spacing, d. Generally an accuracy of 0.005 inches could be expected. If, however, the ice layer grew close to the plexiglass wall multiple echos would be picked up, giving senseless results. The cause for this seemed to be either too great a power input to the transducer for the close proxmity of the ice layer, or else excessive curvature/inclination was present in the ice-water interface.

The ice itself grew very uniform and smooth as evidenced by the time lapse photographs shown in figure 5.1. Since the inlet water temperature possessed little superheat (to = 38 °F), with a relatively low Reynold's number (Re = 250), and a fairly cold coolant temperature (t_b = -10 °F), the ice in the initial seconds grew quite rapidly, eventually causing complete channel blockage. The ice possessing rapid growth is seen in the photographs as a white layer while the slower growing clear ice may be seen near the leading edge of the formation. In general, most of the ice grown during various trial runs tended to be of the latter type.

It has been intended that the design, construction, and eventual testing of the apparatus described in this thesis represent the first step in a program to research the effects caused by solidification occuring when the flow is through an annular passage. Fluid flow between parallel plates being the limiting case of such a flow.

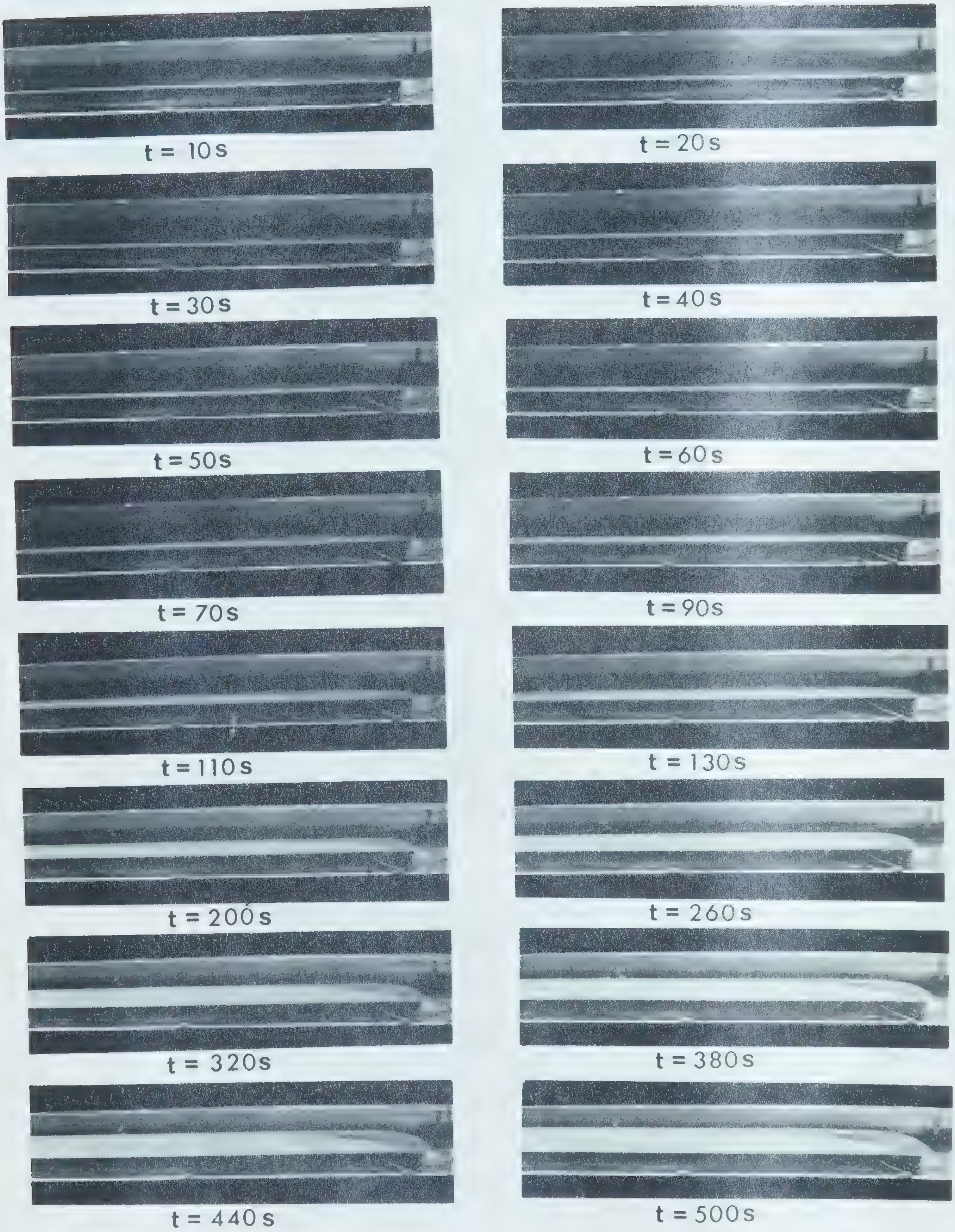

t = 10s

t = 20s

t = 30s

t = 40s

t = 50s

t = 60s

t = 70s

t = 90s

t = 110s

t = 130s

t = 200s

t = 260s

t = 320s

t = 380s

t = 440s

t = 500s

FIGURE 5.1 ICE PROFILE vs TIME

REFERENCES

1. Stefan, J. "uber die Theorie der Eisbildung, insbesondere uber die Eisbildung in Polarmaere," Annalen der Physik und Chemie, Vol. 42, 1891, p. 269.

2. Muehlbauer, J. C. and Sunderland, J.E., "Heat Conduction with Freezing or Melting," Applied Mecnanics Reviews, Vol. 18, No. 12, 1965, p. 951 - 959.

3. Carslaw, H.S. and Jaeger, J.C., "Conduction of Heat in Solids," 2nd Ed. Oxford at the Clarendon Press, 1959, p. 282 - 296.

4. Brush, W.W., "Freezing of Water in Subaqueous Mains Laid in Salt Water and in Mains and Services Laid on Land," Journal of the American Water Works Association, Vol. 3, 1916, p. 962 - 980.

5. Hirschberg, H.G., "Freezing of Piping Systems," Kaltetechnik 14, 1962, p. 314 - 321.

6. Libby, P. A. and Chen, S., "The Growth of a Deposited Layer on a Cold Surface," Int. J. Heat Mass Transfer, Vol. 8, 1965, p. 395 - 402.

7. Goodman, T. R., "The Heat Balance Integral and its Application to Problems Involving a Change of Phase," Trans. ASME, Vol. 80, 1958, p. 335 - 342.

8. Goodman, T. R., "The Heat Balance Integral - Further Considerations and Refinements," Trans. Am. Soc. Mech. Engrs., Vol. 83, 1961, p. 83 - 86.

9. Goodman, T. R., "Application of Integral Methods to Transient Nonlinear Heat Transfer," Advances in Heat Transfer, Vol. 1, (ed. Irvine, T.F. and Hartnett, J.P.) 1964, p. 51 - 122.

10. Lapadula, C. and Mueller, W., "Heat Conduction with Solidification and a Convective Boundary Condition at the Freezing Front," Int. J. Heat Mass Transfer, Vol. 9 (1), 1966, p. 701 - 704.

11. Biot, M. A., "New Methods in Heat Flow Analysis With Application to Flight Structures," J. Aeronautical Sciences, Vol. 24, 1957, p. 857 - 873.

12. Biot, M.A., "Further Developments of New Methods in Heat Flow Analysis," J. Aero/Space Sci., Vol. 26, 1959, p. 367 - 381.

13. Yang, K. T., "Formation of Ice in Plane Stagnation Flow," Appl. Sci. Res., Vol. 17, 1967, p. 377 - 396.

14. Beaubouef, R. T. and Chapman, A. J., "Freezing of Fluids in Forced Flow," Int. J. Heat Mass Transfer, Vol. 10, 1967, p. 1581 - 1587.

15. Zerkle, R. D. and Sunderland, J. E., "The Effect of Liquid Solidification in a Tube Upon the Laminar-Flow Heat Transfer and Pressure Drop," Trans ASME, Vol. 90, 1968, p. 183 - 190.

16. Zerkle, R. D. and Lee, D. G., "The Effect of Liquid Solidification in a Parallel Plate Channel Upon Laminar-Flow Heat Transfer and Pressure Drop," Trans. ASME, Vol. 91, 1969, p. 583 - 585.

17. Siegel, R. and Savino, J. M., "Experimental and Analytical Study of the Transient Solidification of a Warm Liquid Flowing over a Chilled Flat Plate," NASA TN - D - 4015, 1967.

18. Adams, C. M., Jr., "Thermal Considerations in Freezing," Liquid Metals and Solidification, Amer. Soc. for Metals, 1958, p. 187 - 217.

19. Siegel, R. and Savino, J. M., "Transient Solidification of a Flowing Liquid on a Cold Plate Including Heat Capacities of Frozen Layer and Plate," NASA TN - D - 4353, 1968.

20. Savino, J. M. and Siegel, R., "An Analytical Solution for Solidification of a Moving Warm Liquid onto an Isothermal Cold Wall," Int. J. Heat Mass Transfer, Vol. 12, 1969, p. 803 - 809.

21. Gort, C., "Preliminary Study of Ice Formation in a Vertical Pipe," M. Sc. Thesis, University of Alberta, Edmonton, Alberta, June, 1968.

22. DesRuisseaux, N. and Zerkle, R. D., "Freezing of Hydraulic Systems," Paper presented at the AIChE - ASME Heat Transfer Conference and Exhibit, Philadelphia, Pa., August 11 - 14, 1968.

23. Ozisik, M. N. and Mulligan, J. C., "Transient Freezing of Liquids in Forced Flow inside Circular Tubes," Trans. ASME, Vol. 91, p. 385 - 390.

24. Stephan, K., "Influence of Heat Transfer on Melting and Solidification in Forced Flow," Int. J. Heat Mass Transfer, Vol. 12, 1969, p. 199 - 214.

25. Lock, G. S. H., Freeborn, R. D. J., and Nyren, R. H., "Analysis of Ice Formation in a Convectively - Cooled Pipe," Heat Transfer, 1970, Elsevier, Amsterdam, Vol. 1, 1970.

26. Freeborn, R. D. J., "Ice Formation in Vertical Tubes with Convective Boundary Conditions," M. Sc. Thesis, University of Alberta, Edmonton, Alberta, Spring, 1969.

27. Sellars, J. R., Tribus, M., and Klein, J. S., "Heat Transfer in Laminar Flow in a Round Tube or Flat Conduit - the Graetz Problem Extended," Trans. ASME, Vol. 78, 1956, p. 441 - 448.

28. Nyren, R. H., Lock, G. S. H., "Analysis of Fully Developed Ice Formation in a Convectively - Cooled Circular Tube," Third Western Canadian Heat Transfer Conference, University of Alberta, Edmonton, Alberta, 1970.

29. Nyren, R. H., "Asymmetric Ice Formation in Convectively Cooled Pipes," M. Sc. Thesis, University of Alberta, Edmonton, Alberta, Spring, 1971.

30. Bilenas, J. A. and Jiji, L. M., "Numerical Solution of a Non - linear Free Boundary Problem of Axisymmetric Fluid Flow in Tubes with Surface Solidification," Heat Transfer 1970, Elsevier, Amsterdam, Vol. 1, 1970, Variational Solution of Axisymmetric Fluid Flow in Tubes with Surface Solidification," Journal of the Franklin Institute, Vol. 289, 1970, p. 265 - 279.

31. Bilenas, J. A., "Axisymmetric Fluid Flow in Tubes with Surface Solidification," Ph. D. Thesis, City University of New York, 1968.

32. Lazaridis, A., "A Numerical Solution of the Multidimensional Solidification (or Melting) Problem," Int. J. Heat Mass Transfer, Vol. 13, p. 1459 - 1477;see also "A Numerical Solution of the Solidification Problem," Eng. Sc. D., Columbia University, 1969.

33. Bruno, J. A., "Mathematical Study of Some Solid - Liquid Melting and Freezing Problems with Moving Interfaces," Ph. D. Thesis, University of Pittsburgh, 1970.

34. Ostrach, S., "Role of Analysis in the Solution of Complex Physical Problems," 3rd. International Heat Transfer Conference, August, 1966.

35. Han, L. S., "Hydrodynamic Entrance Lengths for Incompressible Laminar Flow in Rectangular Ducts," Journal of Applied Mechanics, Vol. 27, 1960, p. 403 - 410.

36. Bailey, J. A., and Dula, A., "Acoustic Technique for Use in Some Solidification Rate Studies," The Review Science Instruments, Vol. 38, No. 4, Apr. 1967, p. 535 - 538.

APPENDIX A

APPENDIX A

INTEGRAL CONTINUITY EQUATION

Although not strictly necessary for the mathematical formulation of the problem it is worthwhile to introduce an integral form of the continuity equation. Due to the change in pressure and the rate of solidification in the freezing zone, the mass flow is an unknown which must be determined. Thus to ensure that the mass flow is conserved the derived equation must be satisfied.

Consider a control volume of unit width placed around the freezing zone as indicated.

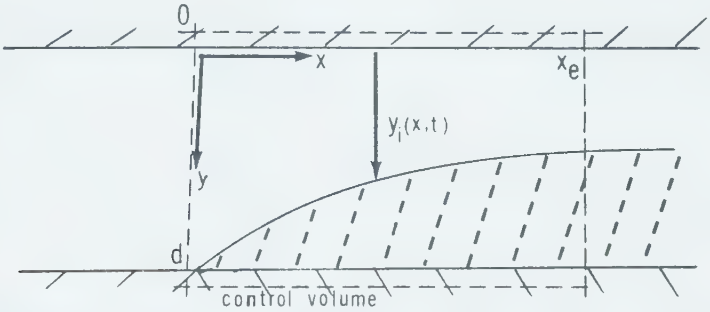

The mass entering the control volume between times t_0 and t is:

$$Mi = \int_{t_0}^{t} \int_{0}^{d} \rho_L u(0, y, t)\, dy\, dt$$

The mass leaving the control volume in the time interval is:

$$Me = \int_{t_0}^{t} \int_{0}^{y_i(x_e t)} \rho_L u(x_e, y, t) dy\, dt$$

The fluid mass initially in the control volume is:

$$M_{if} = \int_0^{x_e} \rho_L \; y_i \; (x, t_o) dx$$

The fluid mass in the control volume at time t is:

$$M_{ff} = \int_0^{x_e} \rho_L y_i \; (x, t) dx$$

The accumulation of solid mass in the time interval is:

$$M_s = \int_0^{x_e} \rho_s \; (y_i \, (x, t) - y_i \, (x, t_o)) dx$$

Since the total mass is conserved then

$$M_s = M_e - M_i + M_{ff} - M_{if}$$

Substituting and rearranging gives:

$$\int_{t_o}^{t} \int_0^{d} u(0, y, t) dy dt - \int_{t_o}^{t} \int_0^{y_i(x_e, t)} u(x_e, y, t) dy \, dt$$

$$= \left(1 - \frac{\rho_s}{\rho_L}\right) \int_0^{x_e} [(y_i(x, t) - y_i(x, t_o)] \; dx$$

Differentiating w.r.t time and formulating in terms of non dimensional quantities gives equation 2.3 - 9

$$\int_0^1 U dY - \int_0^{\eta} U dY = \frac{1-\rho}{\delta\alpha P_e} \int_0^X \frac{\partial \eta}{\partial \tau} dX$$

The equation introduces the additional non-dimensional parameter, ρ , the ratio of the solid to liquid density.

APPENDIX B

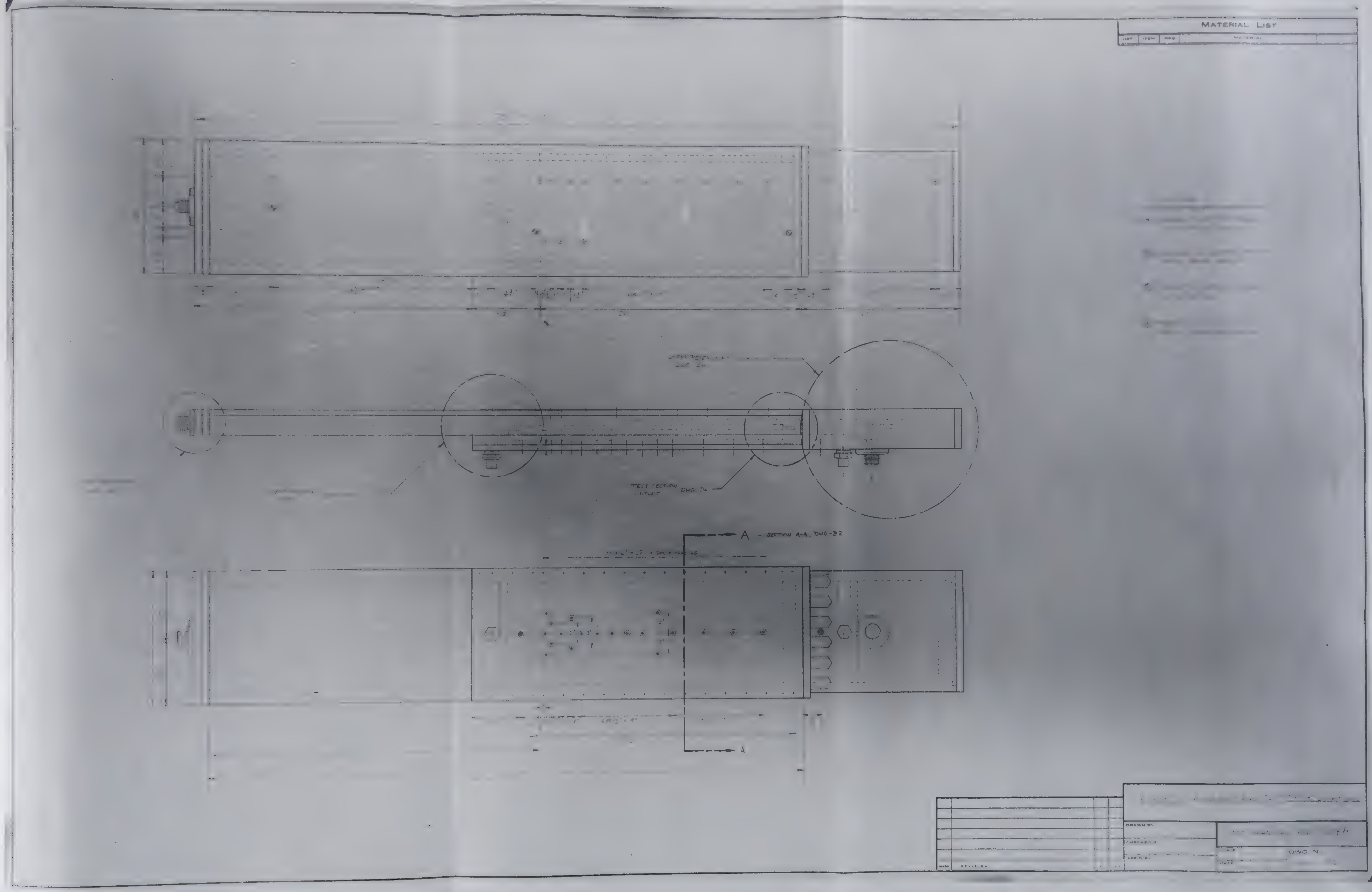
MATERIAL LIST
MATERIAL
TEST SECTION OUTLET
DWG 34
A - SECTION A-A, DWG-32
A
DRAWN BY
CHECKED BY
APP'D BY
DATE
DWG NO

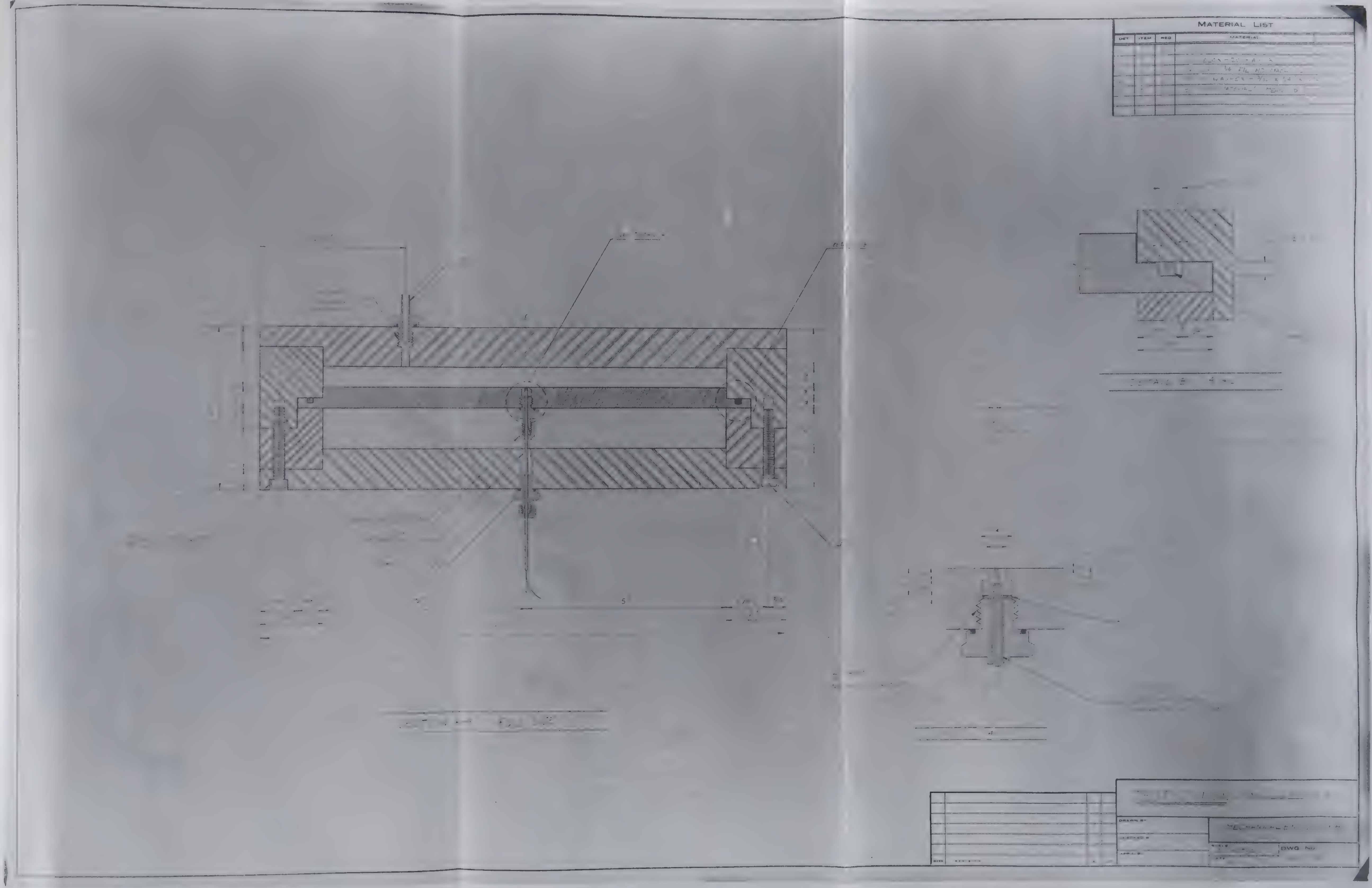
MATERIAL LIST
DET
ITEM
REQ
MATERIAL
1/4
WASHER
5"
DRAWN BY
DWG NO

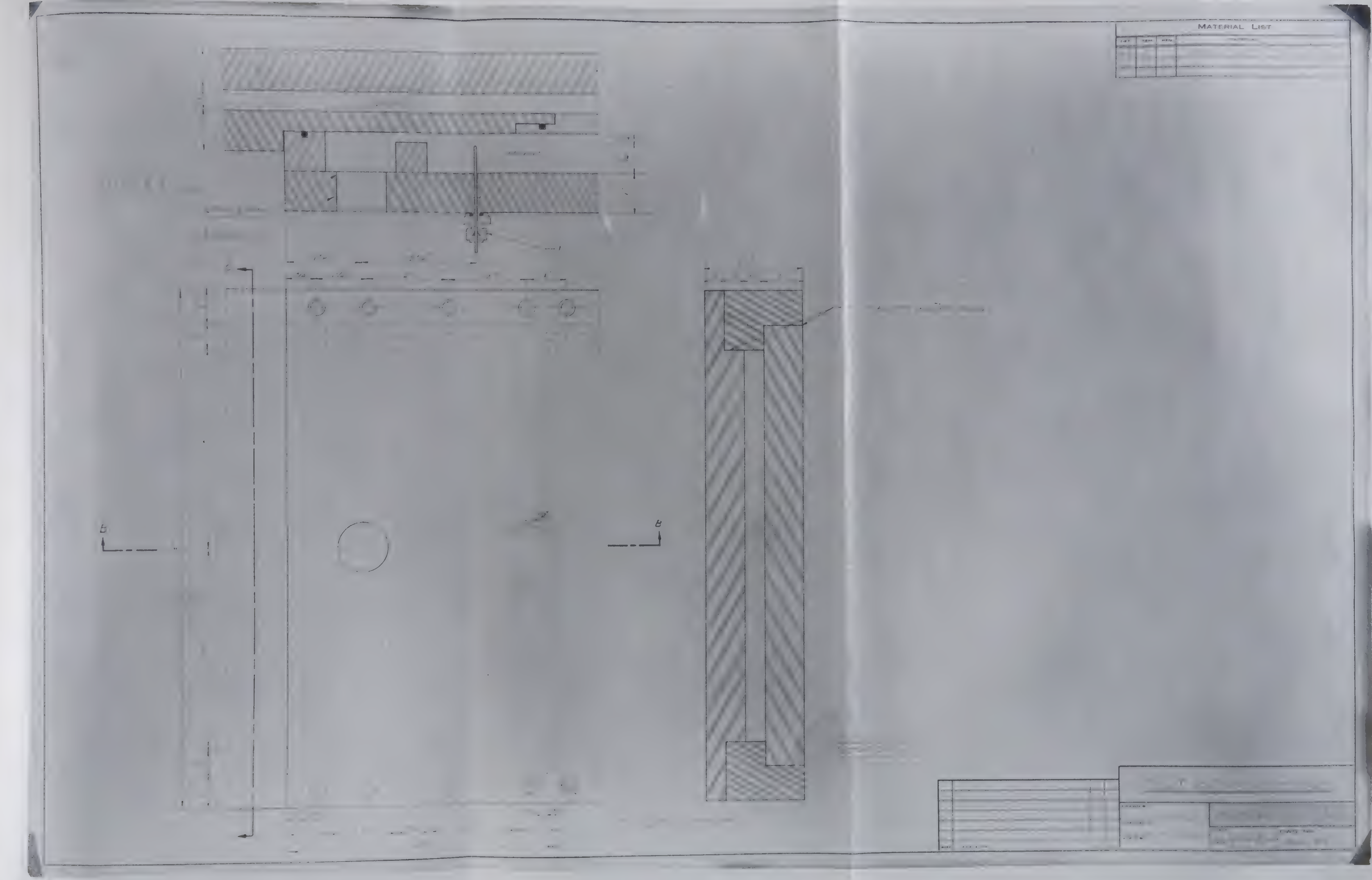
MATERIAL LIST
B
B

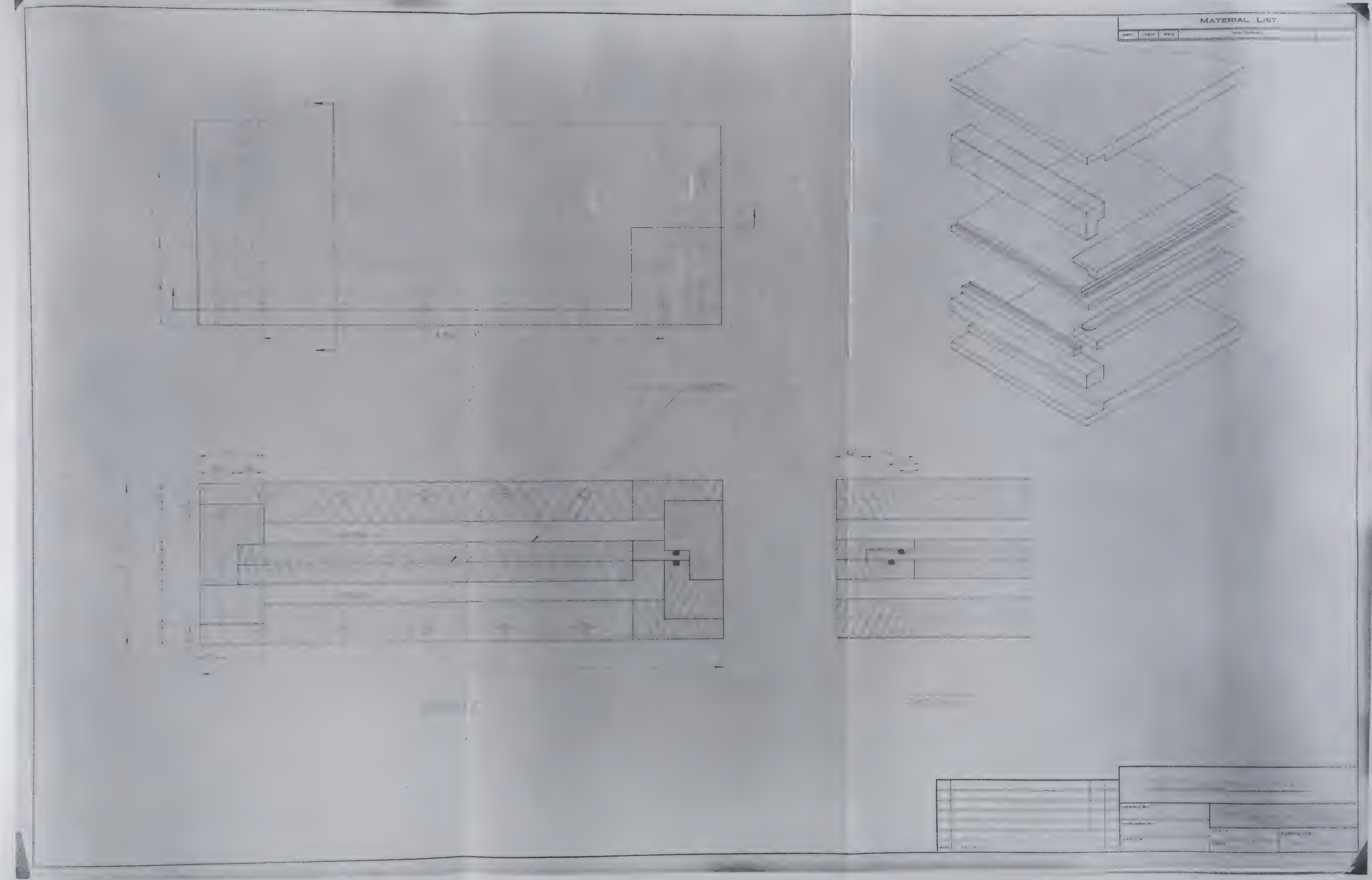
MATERIAL LIST
DET
ITEM
REQ
MATERIAL

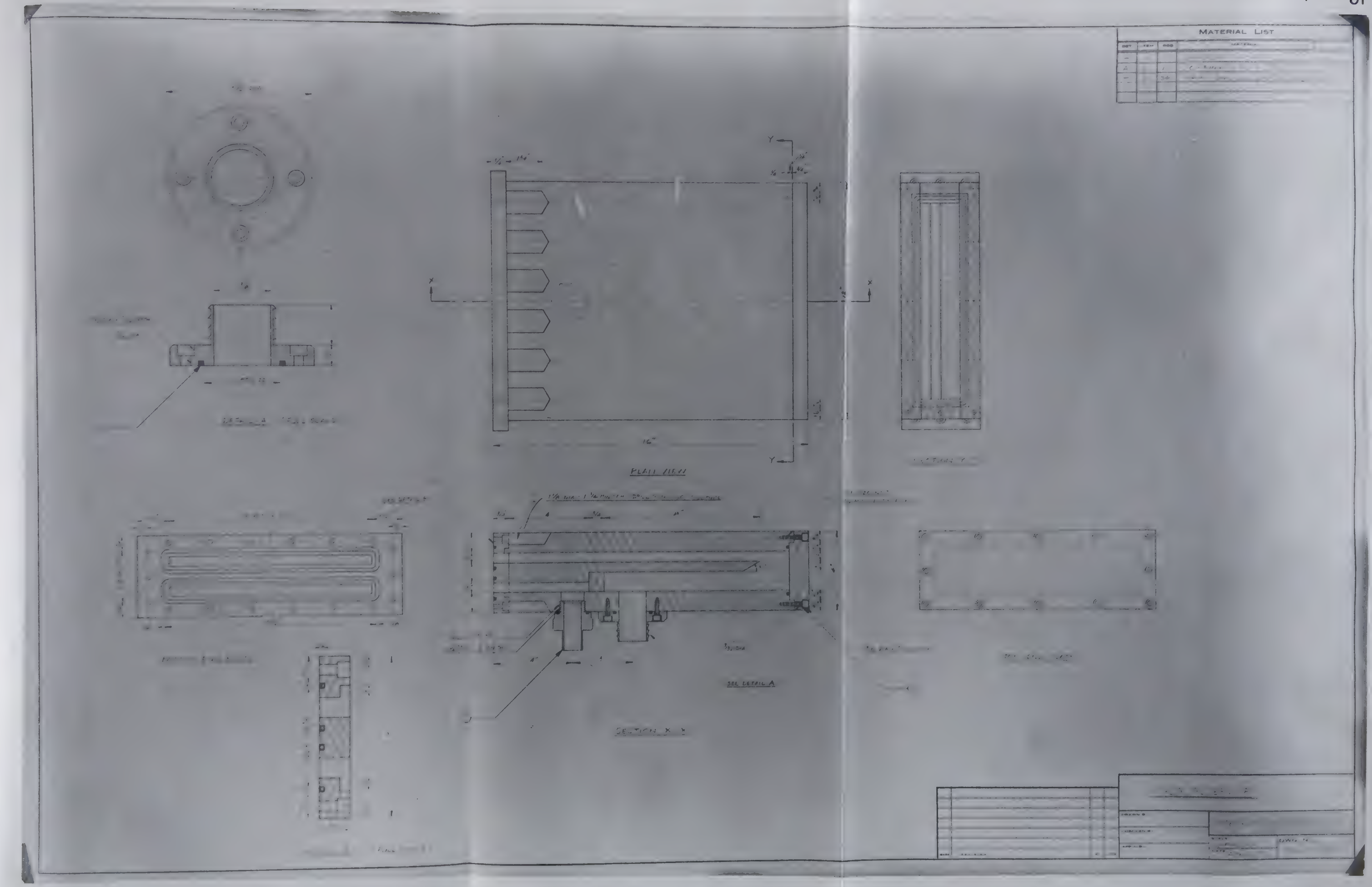
MATERIAL LIST
Y
X
16"
PLAN VIEW
SEE DETAIL A
SECTION X-X

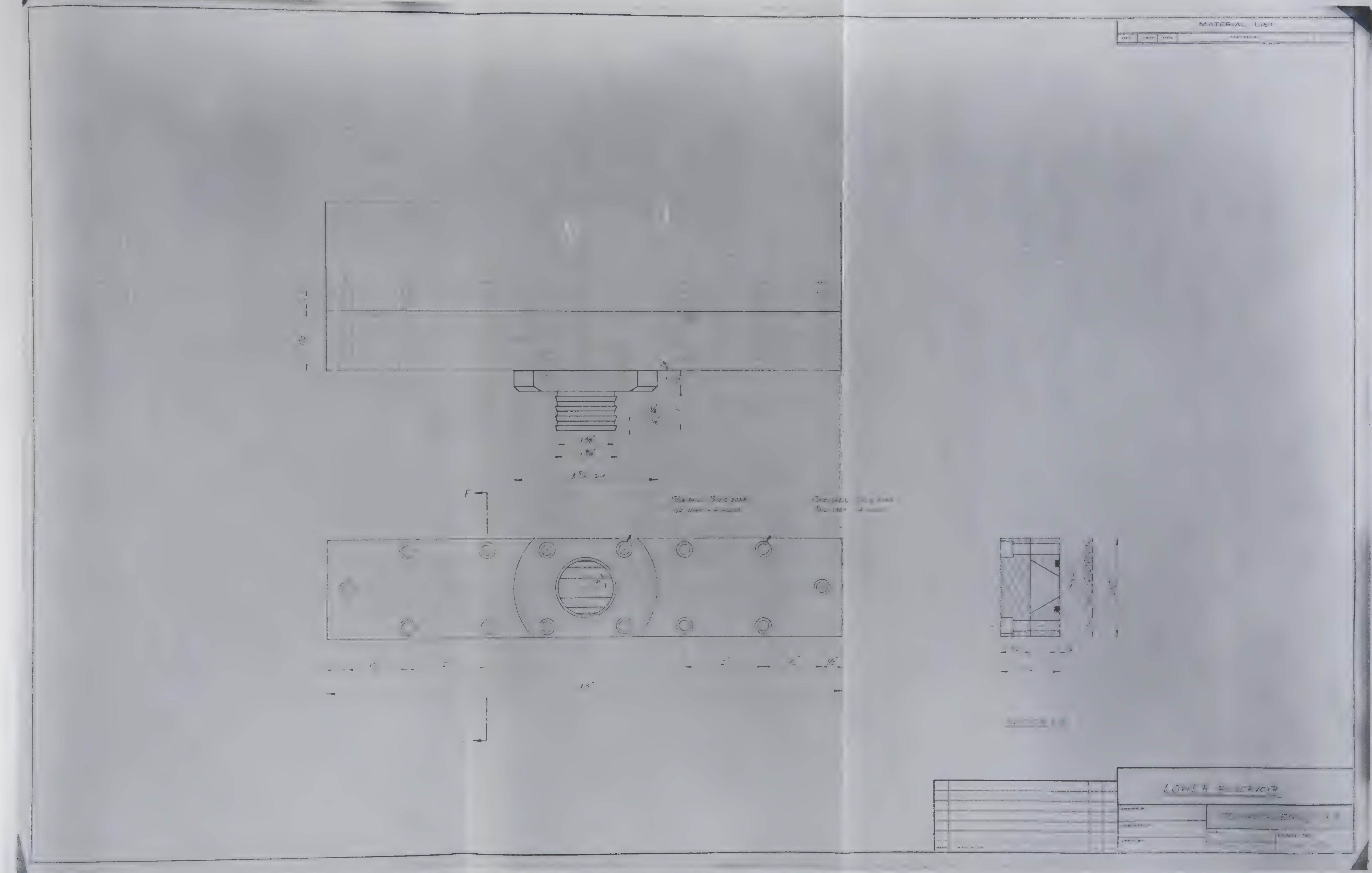
MATERIAL LIST
F
1 3/4"
1 9/16"
3 5/8 DIA
17/64 DRILL 13/32 C'BORE
13"
3"
LOWER RESERVOIR
DRAWN BY

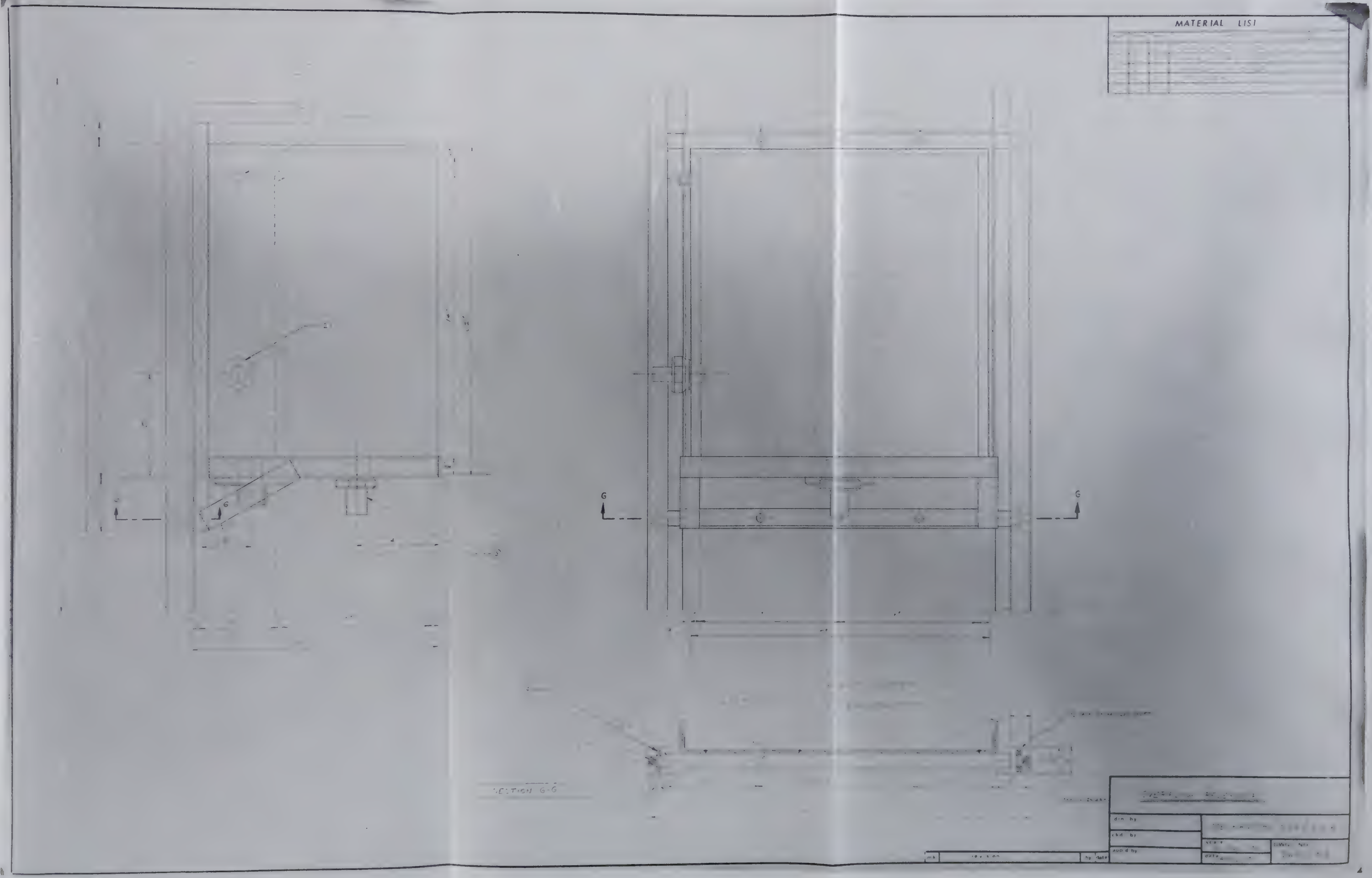
MATERIAL LIST
G
G
G
SECTION G-G
drn by
ckd by
app'd by
scale
date
dwg. no.
mk
revision
by
date

APPENDIX C

APPENDIX C

EQUIPMENT

The following represents a list of the main components used in the preliminary testing of the system.

'Warm Water' Storage	- 150 Imperial gallon insulated storage tank - 2 - 1500 watt Tempro Automatic water heaters - ½ ton - Copland refrigeration unit - 15 IGPM Moyno F S Utility pump - discharge line and return line - 1" diameter flexible tubing
Test Section	- coolant inlet and discharge piping - 1" diameter flexible tubing - 'Warm Water' inlet and discharge lines - 1½" diameter flexible tubing
Cooling System	
Coolant	- Ethylene glycol-water mixture 50/50
Coolant reservoir	- 60 Imperial gallon capacity
Refrigeration unit	- 1½ ton capacity - Copland
Control valve	- Honeywell 1616 Three-Way mixing valve - Modutrol electric motor (M944) actuated - Honeywell proportioning indicating temperature controller T9S4A Range - 50 to 100 °F
Coolant Pump	- 25 IGPM Jabsco
Instrumentation	
Ultrasonic Test Equipment	- Branson Flow and Thickness Tester, Sonoray 600 - Branson Time Base Module, Model 610

Potentiometers	- Honeywell Electronik 15 Strip Chart Multipoint Recorder - Hewlitt Packard X-Y recorder Model 2 D - 2A - Hewlitt Packard Strip Chart recorder, Model 7101B
Turbine Flowmeter	- Brooks Model 4901 - 10 Journal Bearing design - Brook 4300T - Frequency Converter - General Radio - 1192 Counter
Pressure Sensor	- T, E, M, Instrument 36 Channel manometer mercury filled - Canon F-1 35 millimeter single reflex camera, electric motor drive and interval timer - Rosemount Engineering Differential Pressure Transmitter Model 1151DP